AD-A089 439 ADVISORY GROUP FOR AEROSPACE RESEARCH AND DEVELOPMENT--ETC F/G 1/2
MATHEMATICAL MODELING OF LINEAR AND NON-LINEAR AIRCRAFT STRUCTU--ETC(U)
JUL 80
UNCLASSIFIED AGARD-R-687 NL

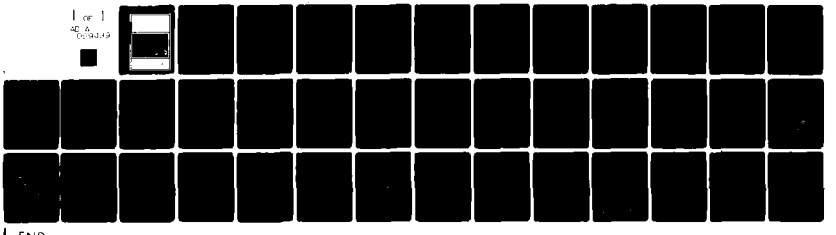

END
DATE FILMED
10-80
DTIC

AGARD-R-687

AGARD-R-687

AGARD

ADVISORY GROUP FOR AEROSPACE RESEARCH & DEVELOPMENT

7 RUE ANCELLE 92200 NEUILLY SUR SEINE FRANCE

AGARD REPORT No. 687

Mathematical Modeling of Linear and Non-Linear Aircraft Structures

NORTH ATLANTIC TREATY ORGANIZATION

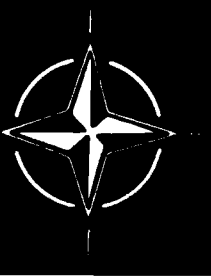

DISTRIBUTION AND AVAILABILITY
ON BACK COVER

AGARD-R-687

NORTH ATLANTIC TREATY ORGANIZATION

ADVISORY GROUP FOR AEROSPACE RESEARCH AND DEVELOPMENT

(ORGANISATION DU TRAITE DE L'ATLANTIQUE NORD)

AGARD Report No.687

MATHEMATICAL MODELING OF LINEAR AND NON-LINEAR AIRCRAFT STRUCTURES

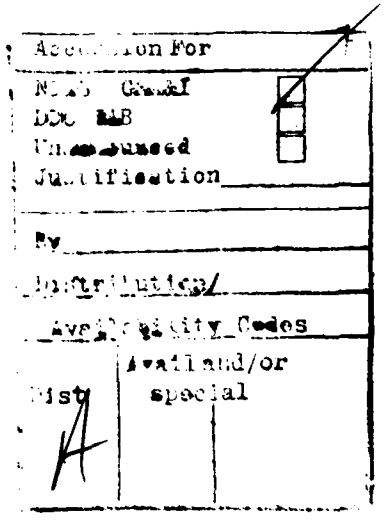

This report was prepared at the request of the Structures and Materials Panel of AGARD.

THE MISSION OF AGARD

The mission of AGARD is to bring together the leading personalities of the NATO nations in the fields of science and technology relating to aerospace for the following purposes:

- Exchanging of scientific and technical information;
- Continuously stimulating advances in the aerospace sciences relevant to strengthening the common defence posture;
- Improving the co-operation among member nations in aerospace research and development;
- Providing scientific and technical advice and assistance to the North Atlantic Military Committee in the field of aerospace research and development;
- Rendering scientific and technical assistance, as requested, to other NATO bodies and to member nations in connection with research and development problems in the aerospace field;
- Providing assistance to member nations for the purpose of increasing their scientific and technical potential;
- Recommending effective ways for the member nations to use their research and development capabilities for the common benefit of the NATO community.

The highest authority within AGARD is the National Delegates Board consisting of officially appointed senior representatives from each member nation. The mission of AGARD is carried out through the Panels which are composed of experts appointed by the National Delegates, the Consultant and Exchange Programme and the Aerospace Applications Studies Programme. The results of AGARD work are reported to the member nations and the NATO Authorities through the AGARD series of publications of which this is one.

Participation in AGARD activities is by invitation only and is normally limited to citizens of the NATO nations.

Published July 1980

ISBN 92-835-1365-7

Printed by Technical Editing and Reproduction Ltd
Harford House, 7–9 Charlotte St, London, W1P 1HD

PREFACE

The mathematical modeling of aircraft structures (for instance by finite elements) is used, from the very beginning of a design, to determine the flutter boundaries and the dynamics of the aircraft. Once the prototype is built, extensive vibration tests take place in order to compare the theoretical prediction with the actual natural modes and frequencies. Discrepancies then appear, especially for wing-store configurations, that must be explained and the mathematical model must be modified to fit the experimental results.

The authors addressed two different aspects of the problem in their presentations at the Spring 1980 Meeting of the Structures and Materials Panel in Athens: In his paper, Zimmermann proposes adjustment algorithms for improving the theoretically obtained flexibility and mass distributions of a structure by dynamic or ground resonance tests. On the other hand, De Ferrari, Chesta, Sensburg and Lotze deal with the non-linear behaviour of wing-store configurations and its analytical representation. They draw clear conclusions on the excitation amplitudes at which flutter could occur.

The two papers provide a very important contribution to the understanding of some difficult aeroelastic problems and will be very useful to the NATO community.

G.COUPRY
Chairman,
Aeroelasticity Sub-Committee

CONTENTS

	Page
PREFACE	iii
OPTIMIZATION OF THE MATHEMATICAL MODEL OF A STRUCTURE by H.Zimmermann	1
EFFECTS OF NONLINEARITIES ON WING-STORE FLUTTER by G.De Ferrari, L.Chesta, O.Sensburg and A.Lotze	15

OPTIMIZATION OF THE MATHEMATICAL MODEL OF A STRUCTURE

by
Helmut Zimmermann
Vereinigte Flugtechnische Werke GmbH, D-2800 Bremen,
Germany

SUMMARY

For the design and certification of aircraft and spacecraft structures the dynamic and flutter behaviour must be well known. Usually the response of such a structure will be represented as a series of the eigenmodes of the structure. The eigenmodes of such a structure will be measured in ground resonance test, but not for all configurations for which calculation'results are necessary. Therefore, calculated modes are used for representing the dynamic and flutter behaviour of the structure, which can be improved by the results of the ground resonance test. In this paper adjustment algorithms are presented for improving the theoretically obtained flexibility- or stiffness- and mass distribution of such a structure by dynamic test or ground resonance test results. The necessary assumptions for the adjustment and the mathematical formalism for the adjustment procedure are given. Experiences gained and adjustment results obtained with these algorithms are reported on concentrating especially on one which uses only the measured and calculated eigenfrequencies. Proposals for improvements on the procedures and in the algorithms are also given.

LIST OF SYMBOLS

A dot over a letter means differentiation with respect to time,
an underlined letter means a vector or a matrix,
a dashed vector or matrix means its transpose,
values of the "Theoretical model" are without index,
values of the "Test Model" have a superscript index M,
values of the "Adjusted Model" have a superscript index K.

$\underline{M}$	Inertia matrix	$\underline{\Lambda}$	Matrix of eigenvalues
$\underline{K}$	Stiffness matrix	a_r	Adjustment parameters
$\underline{C}$	Flexibility matrix	ω_j	Eigenfrequency in radians
$\underline{C}_\varrho$	Flexibility matrix of a substructure	A,G	Weighting matrices
$\underline{Z}$	Vector for the displacement	$\underline{I}$	Unit matrix
$\dot{\underline{Z}}$	Amplitude of the vector for displacement	n	number of degrees of freedom of the "Theoretical Model"
$\underline{f}$	Vector of input forces	$\dot{m}$	number of measurement points
$\underline{X}_j$	Eigenvector	N	number of degrees of freedom of the "Test Model"
$\underline{X}$	Matrix of the eigenvectors	δ_{ij}	Kronnecker Delta
λ_j	Eigenvalue	p	parameter for perturbation

1.o INTRODUCTION

For design and certification of aircraft and spacecraft structures, the dynamic and flutter behaviour must be well known. For describing the dynamic behaviour of a structure the stiffness or flexibility, the structural damping and the mass distribution and the environmental input are necessary. The stiffness and mass distribution of a structure can be calculated more or less exactly from the design drawings. With these calculated distributions the eigenmodes, the eigenfrequencies and the generalized masses of the conservative structure can be determined. Using these eigen-vibration-characteristics and the estimated overall structural damping values the dynamic response of the structure to different environmental inputs can be calculated by the so-called mode methods. With the same methods the dynamic stability problems e.g. flutter are solved.Therefore the eigenvibration characteristics must be improved by measurements results. Measured eigenvibration characteristics are obtained e.g. by the ground resonance test. This test will be done only for certain weight configurations. By improvement of the stiffness- or flexibility- and the mass distribution e.g. by measured eigenvibration characteristics the characteristics for the configurations which are not measured are also improved.

In the past the calculated characteristics were adjusted to the measured ones by trial and error methods. In the last ten years a number of papers were published which give mathematical procedures for adjusting the eigen-vibration-characteristics. Most of them present procedures for improving the calculated stiffness and mass-distribution and only such procedures and the experienceswhich were gained with these will be discussed in this paper.

Two different test results are used to improve the stiffness or flexibility and mass distribution of the structure:

1. the measured eigenvibration characteristics of the structure

2. the measured dynamic response of the structure on a well-defined environmental input

But first the basic conditions and the assumptions made for adjusting theoretical values to measured ones will be mentioned.

2.0 THEORETICAL AND EXPERIMENTAL MODELLING

To get the mathematical equations for calculating the eigen-vibration characteristics of a structure many abstractions must be made in the theoretical model. (see Fig.1):

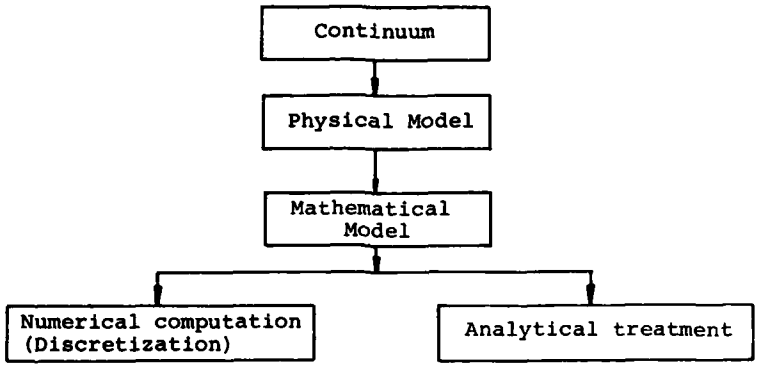

Fig.: 1 Theoretical Model

Usually the present structure, for which the vibration characteristics are to be estimated, is a continuous one. A "Physical Model" for estimating the vibration characteristics of the structure must be extracted by neglecting all details which do not significantly influence the vibration estimation in the required frequency domain. The "Mathematical Model" will be deduced from the "Physical Model" by a mathematical description of this model neglecting unessential details. This "Mathematical Model" is usually solved by numerical computation, which means that a discretization of the continuous structure in the form of a lumped mass system or development of the solution vector in a finite series of well fitted functions must be performed.

The "Test Model" starts with the same "Continuum" as the "Theoretical Model". (see Fig. 2):

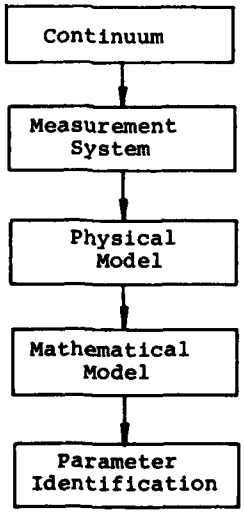

Fig. 2: Test Model

But this "Continuum" is changed by environmental influences, such as measuring and exciting systems, and therefore this will be called the "Measurement System". As in the "Theoretical Model", a "Physical Model" and a "Mathematical Model" are abstracted from the "Measurement System". With this "Mathematical Model" it is possible to do the "Parameter Identification" which means the ascertainment of either the eigenvibration characteristics or the frequency response. A comparison between the theoretical results and the parameter identification results is meaningful only if the "Physical Models" of the "Theoretical"and the "Test Model" are the same. With these assumptions it is possible to improve the theoretical results by parameter identification using the test results.

In this parameter adjustment the disturbances acting on the test model or the sensors play an important role. In Figure 3 the procedure necessary for parameter adjustment is represented. A main point of this paper will be deriving the parameter adjustment algorithms and comparing the possibilities not only for the vibration characteristics such as eigen-frequencies, eigen-modes and so on but also for the structural parameters such as stiffness and masses.

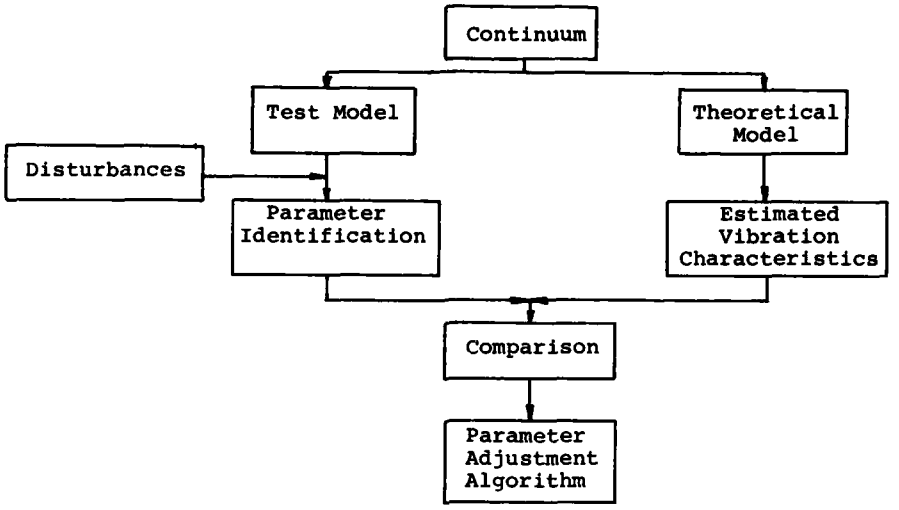

Fig. 3: Parameter Adjustment Configuration

3.o MATHEMATICAL DESCRIPTION

3.1 DESCRIPTION OF THE COMPUTATIONAL MODEL

The computational model is the equations of motion of a discretized elastomechanical system. The system is linear in the sense of classical elastic theory. The structural parameter are assumed to be steady in time and without gyroscopic effects. The structural damping is assumed to be zero or the eigenmodes of the damped system are equal to the eigenmodes of the undamped system. Therefore, only the undamped system will be considered since the damped system will produce no additional because of the assumptions above.

The equations of motion are: $$\underline{M}\ddot{\underline{Z}} + \underline{K}\underline{Z} = \underline{f} \qquad (1)$$

with:

$\underline{M}$: mass matrix, symmetrical, positive definite, real

$\underline{K}$: stiffness matrix, symmetrical, positiv definite or semidefinite, real

$\underline{Z}$: vector of the displacements

$\underline{f}$: vector of the input forces

n : order of matrices

A dot over a letter means differentiation with respect to time.

An underlined letter means a vector or a matrix.

A dashed vector or matrix means its transpose.

To equation (1) there corresponds the eigenvalue equation

$$\underline{C}\,\underline{M}\,\underline{X}_j = \lambda_j \underline{X}_j \tag{2}$$

where $\underline{C} = \underline{K}^{-1}$ is the flexibility matrix,

$\lambda_j = \frac{1}{\omega_j^2}$ with ω_j the eigenfrequency in radians and $\underline{X}_j$ the eigenvector.

With $\underline{\Lambda} = \text{diag}\,\lambda_i$

$\underline{X}' = (\underline{X}_1, \ldots, \underline{X}_n)$ matrix of eigenvectors and

$\underline{M}_G = \underline{X}'\,\underline{M}\,\underline{X} = \underline{I}$ the matrix of generalized masses equation (2) becomes:

$$\underline{X}'\,\underline{M}\,\underline{C}\,\underline{M}\,\underline{X} = \underline{\Lambda} \tag{3}$$

The structural matrices, as mass-, stiffness or flexibility matrices of the defined system, can be represented by the eigenmodes and eigenvalues of the eigenvalue equation (2) as follows:

mass matrix: $$\underline{M} = (\underline{X}\,\underline{X}')^{-1} \tag{4}$$

inverse mass matrix: $$\underline{M}^{-1} = (\underline{X}\,\underline{X}') = \sum_{j=1}^{n} \underline{X}_j \underline{X}_j' \tag{5}$$

stiffness matrix: $$\underline{K} = (\underline{X}')^{-1}\,\underline{\Lambda}^{-1}\,\underline{X}^{-1} \tag{6}$$

flexibility matrix: $$\underline{C} = \underline{X}\,\underline{\Lambda}\,\underline{X}' = \sum_{j=1}^{n} \lambda_j \underline{X}_j \underline{X}_j' \tag{7}$$

3.2 COMPARISON OF VALUES OF THE "THEORETICAL" AND "TEST MODEL"

With equation (4) to (7) it is possible to calculate the mass and stiffness matrices with the measured eigenmodes and to compare the matrices obtained in such a way with the structural matrices used in the "Theoretical Model". It even seems possible to replace the structural matrices calculated from the design drawings by the above-mentioned ones, gained from measured eigenvalues and eigenmodes.

But that is only possible with the following assumptions:

a) The measured and calculated modes must be known at the same positions

b) There must be a one-to-one correspondence between the calculated and measured degrees of freedom.

c) The one-to-one correspondence of the measured and calculated degrees of freedom must be in ascending eigenvalue order.

d) $n = m = N$

with: n : degrees of freedom of "Theoretical Model"

N : degrees of freedom of "Test Model"

m : number of measuring points of the "Test Model"

These assumptions will be fulfilled very rarely. Nevertheless it is possible to compare the structural matrices derived from measured eigenvalues with the theoretical ones. This procedure can be found in [1]. Here only the following should be mentioned:
If all the lower eigenvalues are measured the inverse mass matrix and the flexibility matrix derived from the measured ones give a reasonable approximation because these degrees of freedom are dominant in $\underline{M}^{-1}$ and $\underline{C}$. Therefore, with those assumptions these values could be used for comparison with the theoretical ones.

For the adjustment procedures shown in this paper only the items a) and b) will be assumed, which can be obtained very easily.

a) by suitable selection of the calculated points or by suitable interpolation

and

b) by neglecting those degrees of freedom without one-to-one correspondence between the calculated and measured ones.

3.3 MATHEMATICAL PREPARATIONS

The "Theoretical Model" desribed by equations (1), (2) and (3) shall be improved by the measured result of the "Test Model". For this reason the structural matrices $\underline{M}$ and $\underline{K}$ or $\underline{C}$ have to be adjusted. That is only possible if the structural matrices are functions of the adjustment parameters a_r; r = 1 .... R. Here some relations are derived, which are necessary for setting up the adjustment algorithms the scalars and vectors:

$$\frac{\delta\lambda_i}{\delta a_r} \quad \text{and} \quad \frac{\delta \underline{X}_i}{\delta a_r}$$

Here the eigenvalue equation will be used with the flexibility matrix. In a more general way these scalars and vectors are considered in [2], [3], [4].

From $\underline{X}_i' \underline{M} \underline{X}_i = 1$ it follows that:

$$\frac{\delta \underline{X}_i'}{\delta a_r} \underline{M} \underline{X}_i + \underline{X}_i' \frac{\delta \underline{M}}{\delta a_r} \underline{X}_i + \underline{X}_i \underline{M} \frac{\delta \underline{X}_i}{\delta a_r} = 0 \tag{9}$$

From (2) it follows that:

$$\frac{\delta \underline{C}}{\delta a_r} \underline{M} \underline{X}_i + \underline{C} \frac{\delta \underline{M}}{\delta a_r} \underline{X}_i + \underline{C}\underline{M} \frac{\delta \underline{X}_i}{\delta a_r} = \frac{\delta \lambda_i}{\delta a_r} \underline{X}_i + \lambda_i \frac{\delta \underline{X}_i}{\delta a_r} \tag{10}$$

By premultiplication of (10) with $\underline{X}_i' \underline{M}$ and using the transpose of (2) gives:

$$\frac{\delta \lambda_i}{\delta a_r} = \underline{X}_i' \underline{M} \frac{\delta \underline{C}}{\delta a_r} \underline{M} \underline{X}_i + \underline{X}_i' \underline{M} \underline{C} \frac{\delta \underline{M}}{\delta a_r} \underline{X}_i \tag{11}$$

One simple way of representing $\frac{\delta \underline{X}_i}{\delta a_r}$ is to develop this vector in a series of the eigenvectors of the system:

$$\frac{\delta \underline{X}_i}{\delta a_r} = \sum_{j=1}^{N} \alpha_{ij} \underline{X}_j \tag{12}$$

By multiplying equation (10) $\underline{X}_j' \underline{M}$ with $j \neq i$ from the left, it follows that:

$$\underline{X}_j' \underline{M} \frac{\delta \underline{C}}{\delta a_r} \underline{M} \underline{X}_i + \underline{X}_j' \underline{M} \underline{C} \frac{\delta \underline{M}}{\delta a_r} \underline{X}_i = \underline{X}_j \underline{M} \frac{\delta \underline{X}_i}{\delta a_r} (\lambda_i - \lambda_j) \tag{13}$$

With (12) the right side of (13) will be:

$$(- \lambda_j + \lambda_i) \alpha_{ij}$$

or:

$$\alpha_{ij} = \frac{\underline{X}_j' \underline{M} \frac{\delta \underline{C}}{\delta a_r} \underline{M} \underline{X}_i + \underline{X}_j' \underline{M} \underline{C} \frac{\delta \underline{M}}{\delta a_r} \underline{X}_i}{\lambda_i - \lambda_j} \tag{14}$$

with $i \neq j$

From (9) and with (12) for j = i it follows that:

$$\alpha_{ii} = -\frac{1}{2} \underline{X}_i' \frac{\delta \underline{M}}{\delta a_r} \underline{X}_i \tag{15}$$

With (14) and (15) the α_{ij} in (12) are determined.

Equation (11) and (12) give the wanted expressions for:

$$\frac{\delta \lambda_i}{\delta a_r} \qquad \frac{\delta \underline{X}_i}{\delta a_r}$$

Corresponding expressions can be obtained by replacing the flexibility matrix $\underline{C}$ with the stiffness matrix $\underline{K}$.

3.4 PARAMETER ADJUSTMENT ALGORITHMS

There are two different methods for improving the "Theoretical Model" by "Test Models". The first is to compare calculated and measured dynamic responses of a dynamic system and to adjust the mass matrix and the stiffness matrix of the system directly without using the eigenvalues of the system. This way of improving the flexibility and mass matrix of a structural dynamic system corresponds to the problem of measuring loads and improving calculated loads of an aircraft from its response to known control inputs. These methods are reported for example in [5] , [6] .

Here a similar method is reported which does not work in the time domain as the previously mentioned methods but in the frequency domain [7] .

The algorithm is derived from equation (1), with the force f sinusoidal in time. With $\underline{f} = e^{i\cdot\omega\cdot t}\,\hat{\underline{f}}$ and $\underline{Z} = e^{i\cdot\omega\cdot t}\,\hat{\underline{Z}}$ one obtains from (1):

$$(-\omega^2\underline{M} + \underline{K})\,\hat{\underline{Z}} = \hat{\underline{f}} \tag{16}$$

With $\hat{\underline{Z}}_i^M$, $\hat{\underline{Z}}_i^K$ the measured and calculated responses respectively of the dynamic system for different frequencies ω_i , i: 1, ... S , one obtains with the least square method:

$$\sum_{i=1}^{S} (\hat{\underline{Z}}_i^K - \hat{\underline{Z}}_i^M)'\underline{G}(\hat{\underline{Z}}_i^K - \hat{\underline{Z}}_i^M) = \text{Min}(a_r) \tag{17}$$

With a weighting matrix $\underline{G}$ assumed to be positive definite; a_r are the parameters for adjusting the matrices $\underline{M}$ and $\underline{K}$; S the number of the used exciting frequencies.

Expressing $\hat{\underline{Z}}_i^K$ in (17) in terms of (16) one obtains:

$$\sum_{i=1}^{S}\{\hat{f}_i(-\omega_i^2\underline{M}^K + \underline{K}^K)^{-1} - \hat{\underline{Z}}_i^M\}'\underline{G}\{\hat{f}_i(-\omega_i^2\underline{M}^K + \underline{K}^K)^{-1} - \hat{\underline{Z}}_i^M\} = \text{Min}(a_r) \tag{18}$$

Equation (18) means that the parameters a_r must be chosen in such a way, that the expression becomes a minimum.

The second method for improving the "Theoretical Model" by the "Test Model" is to compare calculated and measured eigenfrequencies and eigenmodes and to find algorithms on this basis. One can obtain cost functions containing measured and calculated frequencies and modes, but those cannot be developed using logic similar to equation (17). Here two different cost functions shall be mentioned:

The first [8] is:

$$\sum_{ij}^{N'}[(\underline{X}_j^K)'\underline{A}\,\underline{X}_j^K\lambda_j^K - (\underline{X}_j^M)'\underline{A}\,\underline{X}_j\lambda_j^M]^2 g_{ij} = \text{Min}(a_r) \tag{19}$$

A and G with the elements a_{ij} and g_{ij} are weighting matrices assumed symmetrical and positive definite. The other values are defined on page 4 . The physical dimension of the expression is power.

The second [9] is:

$$\sum_{j=1}^{N''}(\underline{X}_j^K - \underline{X}_j^M)\,g_j(\underline{X}_j^K - \underline{X}_j^M) + \sum_{j=1}^{N'}(\lambda_j^K - \lambda_j^M)^2 = \text{Min}(a_r) \tag{20}$$

Where the g_j are the elements of a diagonal weighting matrix assumed to be semidefinite and $N \geq N' \geq N''$.

In [4] Natke discusses different cost functions for an adjusting algorithm for dynamic systems. The different cost functions were compared with respect to computational expense and other advantages or disadvantages.

A second method for comparing and adjusting calculated and measured eigenfrequencies and eigenmodes is the statistical system identification [10] , [11] . Definitions for the variances of the parameter a_r of the "Theoretical Model" and variances for the measured eigenvalues leads to an optimal estimation of the parameters a_r with the assumption of normally distributed values for the parameters and normally distributed measured values. The latter adjusting algorithm is comparable to that of the cost function but better founded mathematically.

Several different methods for finding the parameters a_r, which minimize the equations or cost functions (18), (19) or (20) are commonly used. Well known are the "Steepest Descent Method" and the "Newton-Raphson Method". For the latter different versions exist.

If the cost function is denoted by $J(a_1 \ldots a_R)$, it is necessary for each method to know the derivatives:

$$\frac{\delta J}{\delta a_r} \qquad r: \; 1 \ldots R \tag{21}$$

and often also the second derivatives:

$$\frac{\delta^2 J}{\delta a_r \, \delta a_s} \qquad r,s: \; 1 \ldots R \tag{22}$$

The derivatives of (21) and (22), can be expressed in terms of

$$\frac{\delta \lambda_i}{\delta a_r} \quad \text{and} \quad \frac{\delta \underline{X}_i}{\delta a_r}$$

The first term is given by equation (11) and the second term by equation (12) in combination with (14) and (15). Therefore the paper contains all formulas to express the gradients for a given cost function and with the methods indicated it is possible to obtain the required parameters a_r.

Normally the matrices $\underline{M}$ and $\underline{K}$ or $\underline{C}$ are linear functions of a_r, the system of equations

$$\frac{\delta J}{\delta a_r} = 0 \qquad r: \; 1 \ldots R \tag{23}$$

is linear in a_r. By solving this system of equation one obtains a set of the parameters a_r. But equations (11) and (12) show that the eigenvalues and eigenvectors are indirectly functions of the parameter a_r. Therefore the actual parameters a_r can only be obtained by an iterative process as shown in Figure 4. This Figure contains the whole mathematical procedure for adjusting the structural matrices to measured frequency responses or eigenvalues of the dynamic system.

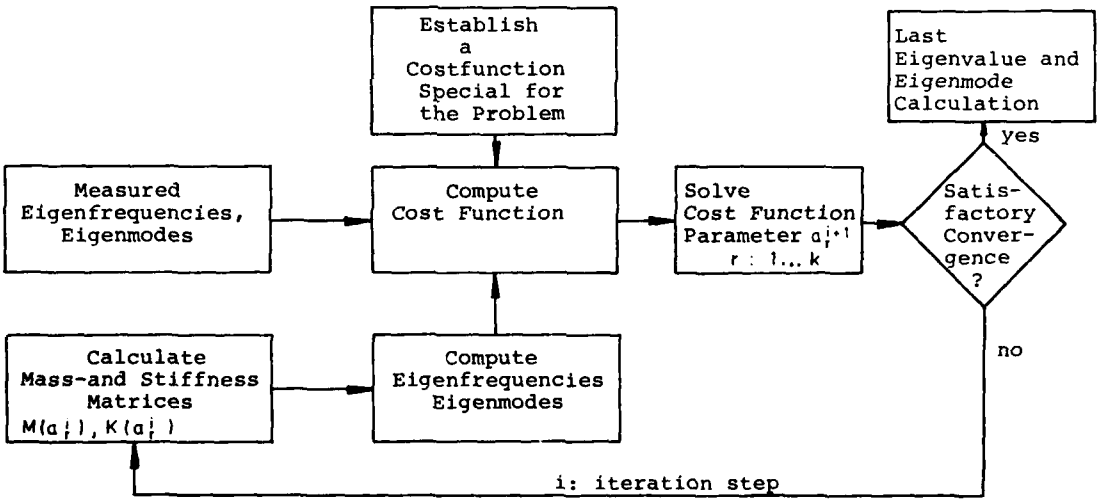

Fig. 4: Computational process for Adjusting the Dynamic System to Test Results

4.0 APPLICATION WITH A SPECIAL COST FUNCTION

4.1 MATHEMATICAL INTRODUCTION

For the application of this adjustment method we have used the cost function (19) with $\underline{A} = \underline{M}$ and $g_{ij} = g_i \delta_{ij}$. With this simplification the cost function in (19) becomes:

$$J(a_1 \ldots a_R) = \sum_{i=1}^{N'} (\lambda_i^K - \lambda_i^M)^2 g_i = \text{Min}(a_r)$$

With this simplification we only use the measured eigenfrequencies and not the measured modes for adjusting the theoretical dynamic system.

Because of the fact that the mass matrix can be calculated nearly exactly, only the flexibility matrix $\underline{C}$ was a function of the parameters a_r. That means:

$$\frac{\delta \underline{M}}{\delta a_r} = 0 \tag{25}$$

To find the parameter dependency of the flexibility matrix, we divided the structure into a number of substructures and multiplied the flexibility matrix of each substructure with the parameter a_r, as:

$$\underline{C} = \sum_{r=1}^{R} a_r \, \underline{C}_r \qquad r: 1 \ldots R \tag{26}$$

The matrices $\underline{C}_r$ have the same order as $\underline{C}$. Rows and columns are filled up with zeros. With these assumptions, we get the following system of equations for determining the parameters a_r.

$$\sum_{i=1}^{N'} (\lambda_i^K - \lambda_i^M) \, g_i \frac{\delta \lambda_i^K}{\delta a_r} = 0 \qquad r: 1 \ldots R \tag{27}$$

With the assumptions above and taking into account equations (3) and (11), equation (12) becomes:

$$\sum_{i=1}^{N'} g_i \left\{ (\underline{X}_i^K)' \underline{M} \left[\sum_{j=1}^{R} a_j \, \underline{C}_j \right] \underline{M} \, \underline{X}_i^K - \lambda_i^M \right\} (\underline{X}_i^K)' \underline{M} \, \underline{C}_r \, \underline{M} \, \underline{X}_i^K = 0 \tag{28}$$

With the definitions:

$$B_{ji} = (\underline{X}_i^K)' \, \underline{M} \, \underline{C}_j \, \underline{M} \, \underline{X}_i \qquad \begin{matrix} j: 1 \ldots R \\ i: 1 \ldots N' \end{matrix}$$

$\underline{G}$: diagonal matrix with the elements g_i, $i: 1 \ldots N'$

$\underline{\lambda}_i^M$: vector with the elements λ_i^M, $i: 1 \ldots N'$

$\underline{a}$: vector with the elements a_r, $r: 1 \ldots R$

equation (28) becomes:

$$\underline{B} \, \underline{G} \, \underline{B}' \, \underline{a} - \underline{B} \, \underline{G} \, \underline{\lambda}^M = 0 \tag{29}$$

Equation (29) is a system of R equations for the parameters a_r. R must be smaller than N' and also smaller than the number of the structural elements and their linear independent displacements.

The adjustment of the "Theoretical Model" to measured eigenfrequencies is performed as shown in Fig. 4. For several examples we did not obtain convergence for this procedure. Therefore we used the parameter perturbation method. We replaced the measured eigenfrequencies λ_i^M by an expression equal to:

$$\frac{\lambda_i^M - \lambda_i^K}{p} \, s + \lambda_i \tag{30}$$

where p is a natural number and s takes sequentially the values 1, ..., p . For s = 1 the value of (30) is close to λ_i^K and for s = p the value of (30) is equal to λ_i^M.

With a suitable p we obtained a mathematical convergent procedure according to the schematic in Fig. 4 with a second iteration process for s = 1,...,p according to equation (30).

In this paper the flexibility matrix is adjusted. For the stiffness matrix there exist a similar procedure. By definition of $\lambda_i = \frac{1}{\omega_i^2}$ in the cost function (24) for the flexibility matrix the lower eigenfrequencies are more highly weighted. For a statically undefined structure the stiffness matrix is more advantageous. With a similar procedure, using a cost function for improving the stiffness matrix, adjustment calculations were made for the skylab structure [12] .

4.2 SYSTEM WITH 14 DEGREES OF FREEDOM

Sample calculations are shown for a system with 14 degrees of freedom, consisting of 14 masses and springs (see Fig. 5), where the spring stiffnesses k_i and the masses m_i have been set to unity for all i = 1, ..., 14.

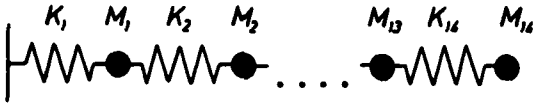

FIG.5 14-degree-of-freedom oscillator

Let the total system be divided into three substructures (R = 3), which consist of masses m_1 to m_4, m_5 to m_8, and m_9 to m_{14}. Let their flexibility matrices be called C_1, C_2 and C_3. This spring-mass oscillator represents the "Theoretical Model". The corresponding "Test Model" is made up of masses m_i = 1, and the flexibility matrix.

$$C = o,6\ C_1 + 1.3\ C_2 + o,8\ C_3$$

In the adjustment calculations four as well as eight degrees of freedom are considered for the cost function. The results are the same for the correction factors a_i of the flexibility matrices.The introduction of large weighting factors did not affect the results. Nor did the choice of a substructure correction factor that was applied a priori to the value to be corrected bring about any changes in the results. The solid curves in Fig. 6 show the dependence of the correction factors on the number of iterations.

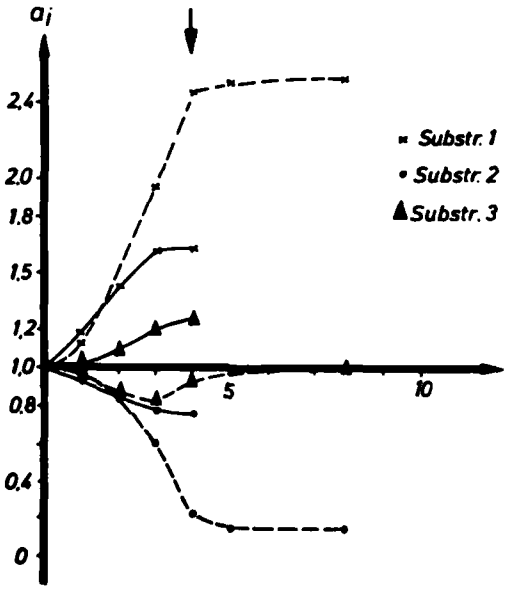

FIG. 6 Convergence of a_i values of the 14-degree-of-freedom oscillator for two different measurement models

In order to simulate measurement errors in the eigenfrequencies for this example, the second eigenfrequency was arbitrarily raised by 15% and the third lowered by 15% in the "Test Model". The dotted lines in Fig. 6 represent the variation of the a_r values with number of iterations. Because of this maladjustment the measurement model and the mathematical model are no longer compatible physically.

Because of the changed "Test Model" the correction values change, and the results of the corrected "Theoretical Model" converge toward the falsified "Test Model". In this simple example this incompatibility shows up as follows:

1. The results of the example did not converge without the application of the perturbation iteration. In order to attain convergence, the number of iterations p in Eq . 3o had to be $p \geq 2$ for the changed system of equations.

2. The number of iterations to attain convergence is larger than in the examples, where mathematical and measurement model are compatible.

3. The eigenvalues resulting from the optimization deviate up to 17% from the initial values.

4.3 APPLICATION TO THE VFW 614

With the same method calculations were made for the adjustment of the eigenmode shapes of the Short Haul Aircraft VFW 614.

In the mathematical model substructures such as fuselage, wing, horizontal and vertical tail were approximated by beams. (see Fig. 7). Attaching these beams to each other was accomplished by means of attachment stiffnesses from Finite Element calculations.

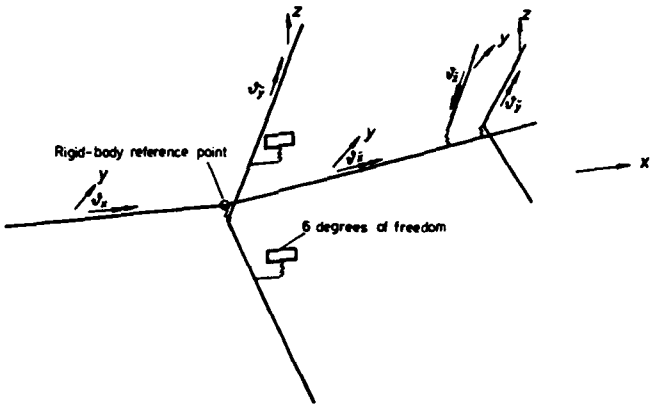

FIG.7 Idealization of the VFW614 structure without control surfaces by a beam model

For the adjustment calculation the aircraft was divided into ten substructures, i.e. RUV - front fuselage, RUH - rear fuselage, FLA - wing attachment, Fl_z - wing bending, Fl_ϑ - wing torsion, HLFA - horizontal tail attachment, HLF_z - horizontal fin bending, HLF_φ - horizontal fin torsion, TRW - engine attachment, SLA - vertical tail attachment (for vertical-tail in-plane oscill'n).

Before results are described, the following terminology will be defined: "Variable Substructures" are those for which the factors a_r of Eqs. (29) are calculated. "Constant Substructures" are characterized by given fixed values of a_r in the solution of Eqs. (29).

In order to get a better insight into the method a simulated "Test Model" was used at first; i. e. for the adjustment calculations eigenmode values were used obtained from eigenmode calculations in which the flexibility matrix for the substructures mentioned above were multiplied by factors not equal to unity. Further adjustment calculations were based on eigenfrequencies measured in the ground vibration test. If the simulated "Test Model" is used the physical models of the "Theoretical" and the "Test Model" are compatible.

Firstly, an adjustment calculation with a simulated "Test Model" is presented. In this calculation all listed substructures except vertical tail and engine attachment are kept variable. From the measurement model 2o eigenfrequencies are known. Figure 8 shows the values of a_r for the various substructures vs. the iteration steps. The a_r values converge to the desired values. The convergence is monotonous except for the horizontal tail attachment. The non-linear system of equations was solved by the parameter perturbation method. The number p-1 of the iterations with altered systems of equations was four just as in the following example. In the diagrams p is marked by an arrow.

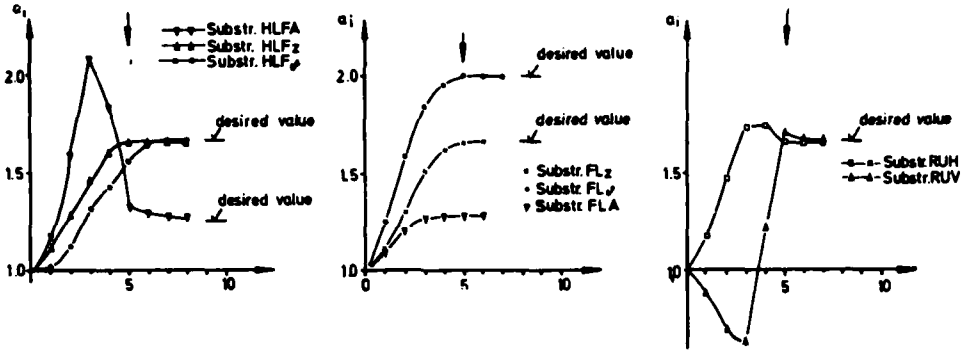

FIG.8 Convergence of the a_i-values for the VFW614 with an input of 20 eigenfrequencies of the compatible measurement model

By reducing the number of the measured eigenfrequencies to ten for the adjustment calculations convergence difficulties appear, because the values for the eigenfrequencies which must be adjusted are much higher than the values of the eigenfrequencies of the "Test Model".

Since arbitrarily high eigenfrequencies cannot be measured during ground vibration tests for reasons of time as well as because of experimental difficulties, the example presented so far and the following one show that one has to be very careful in the choise of the variable substructures, making the most of the available frequency spectrum of the measurement model.

In the following example the eigenfrequencies measured in the ground vibration test were chosen. This example again illustratesthe necessity of a sufficiently large frequency spectrum, and beyond this it also showsthe problems that occur if the physical models of the measurement and the mathematical model are not compatible.

The examples indicate the sensitivity of the results of the adjustment calculation against the experimentally determined eigenfrequency of the 4-node bending of the wing. Setting the frequency of the 4-node wing bending mode to 18.5 Hz yields the following results:

In the first calculation Fl_z, Fl_φ, and HFl_z are variable substructures. Figure 9 shows the variation of the a_r and the significant frequencies against the numver of iterations. It can be seen here that the eigenfrequency of the 4-node wing bending mode converges toward 19.o Hz away from the measured value of 18.5 Hz. In a calculation with the variable substructures RUV and RUH the wing frequencies do not vary with the number of iterations. The factors a_r for the substructures RUV and RUH however deviate so much from unity that ultimately flexibilities are produced that appear to be unrealistic (see Fig. 8). When setting the 4-node wing bending frequency to 18 Hz the adjusted frequency converges toward 18.2 Hz, and the a_r values for the fuselage substructures differ only insignificantly from unity.

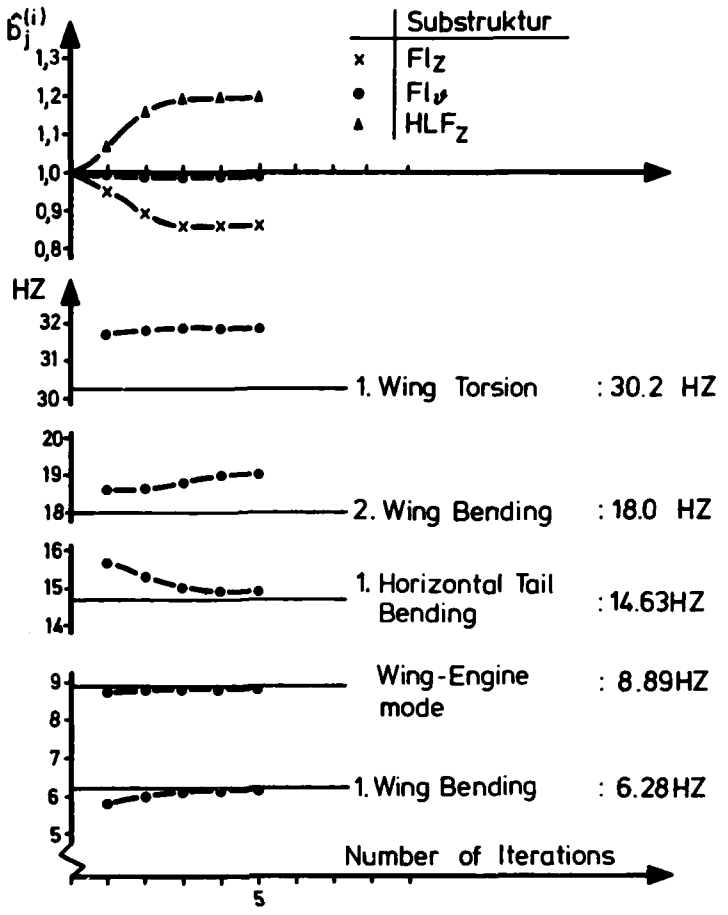

FIG.9 Convergence of the a_i-values and eigenfrequencies against number of iterations when using measured VFW614 eigenfrequencies

To sum up: If the physical systems of the mathematical and measurement models are not compatible, or if the initial corrections are improperly chosen, then convergence may not occur, or the results of the extremum problem do not make sense.

5.0 CONCLUSIONS

The results of the adjustment calculation for symmetrical vibration modes show:

1. There should be a one-to-one correspondence between the degrees of freedom of the mathematical and the measurement model, that are used in the adjustment calculation. If uncertainties exist about the correspondence of certain degrees of freedom, these should be omitted.

2. The frequency spectrum of the measurement model must cover all frequencies to be adjusted. A substructure may be made variable only if an eigenfrequency significant for the substructure is taken from the measurement model.

3. The simultaneous treatment of substructures, during which alterations in their flexibilities lead to different orders of magnitudes in the eigenfrequency shift, result in convergence difficulties.

4. Major incompatibilities between the physical systems of the mathematical and measurement models should be avoided, since they lead to convergence problems.

Further research and considerations give following answers:
Convergence difficulties did appear mainly for attachment substructures. Sometimes if attachment are changed the corresponding eigenfrequencies are changed very little, but the alterations in the nodal line are very big.

Therefore, if substructures for the adjustment procedure are selected, variation calculations for the parameter a_τ of each substructure show their influence on the eigenfrequences and nodal lines of the degrees of freedom of the "Theoretical Model". If there is no influence of one substructure either on the eigenfrequency nor on the nodal line of each degrees of freedom, the corresponding parameter a_τ can be set to unity. If there are bigger influences on the nodal line and lesser influences on the eigenfrequency of a certain degree of freedom, for these degrees of freedom the eigenmodes must be taken into account in the adjustment algorithm.

REFERENCES

[1] H.G. Natke, D. Collmann, H. Zimmermann

Beitrag zur Korrektur des Rechenmodells eines elastomechanischen Systems anhand von Versuchsergebnissen.

VDI-Berichte Nr. 221, 1974

[2] L.A. Kiefling

Comment on "The Eigenvalue Problem for Structural Systems with Statistical Properties".

AIAA Journal 8 (197o), S. 1371 - 1372

[3] R.L. Fox, M.P. Kapoor

Rates of Change of Eigenvalues and Eigenvectors.

AIAA Journal 6 (1968), S. 2426 - 2429

[4] H.G. Natke

Vergleich von Algorithmen für die Anpassung des Rechenmodells einer schwingungsfähigen Struktur an Versuchswerte.

ZAMM 59, 257 - 268 (1979)

[5] A.J. Ross

Application of Parameter Identification Techniques to Analysis of Flight Data

Prog. Aerospace Sci., Vol. 18, pp 325 - 35o
Pergamon Press, 1979

[6] W. Kortüm

Computational Techniques in Optimal State-Estimation - A Tutorial Review

Journal of Dynamic Systems, Measurement and Control,
June 1979, Vol. 1o1/99

[7] H.G. Natke

Die Korrektur des Rechenmodells eines elastomechanischen Systems mittels gemessener erzwungener Schwingungen.

Ingenieur-Archiv 46 (1977) 169 - 184

[8] H. Zimmermann, D. Collmann, H.G. Natke

Erfahrungen zur Korrektur des Rechenmodells mit gemessenen Eigenfrequenzen am Beispiel des Verkehrsflugzeuges VFW 614.

Z. Flugwiss. Weltraumforsch. 1 (1977), Heft 4

[9] B.M. Hall, E.D. Calkin, M.S. Sholar

Linear Estimation of Structural Parameters from Dynamic Test Data.

AIAA/ASME 11th Structures, Structural Dynamics and Material; Conference, Denver, Colorado 197o

[1o] J.D. Collins, W.T. Thomson

The Eigenvalue Problem for Structural Systems with Statistical Properties.

AIAA Journal, Vol. 7, No 1, April 1969

[11] J.D. Collins, G.C. Hart, T.K. Hasselman, B. Kennedy

Statistical Identification of Structures.

AIAA Journal, Vol. 12, No 2, Febr. 74

[12] J.E. Taylor

Sealing a Discrete Structure Model to Match Measured Model frequencies.

AIAA Journal, Vol. 15, No 11

EFFECTS OF NONLINEARITIES ON WING-STORE FLUTTER

by

G. De Ferrari, L. Chesta

AERITALIA
Gruppo Velivoli Da Combattimento
Corso Marche 41, 10146 Torino
Italy

and

O. Sensburg, A. Lotze

MESSERSCHMITT-BÖLKOW-BLOHM GMBH
Airplane Division
P.O.Box 80 11 60, 8000 Munich 80
W.-Germany

ABSTRACT

The effects of structural nonlinearities, in particular friction and backlash, on the dynamic behaviour of airplanes can be very important for flutter. Large nonlinearities do exist on sweepable wing airplanes with sweepable wing mounted stores because a considerable amount of joints (with possible play) and bearings (with play and friction) is necessary but the problem is also present for fixed wing airplanes. A major problem is the interpretation of linear ground resonance and flight flutter tests and their comparison with analytical predictions.

In this paper findings from ground resonance tests and flight flutter tests are presented and an explanation for these test results is given. Calculations with linear assumptions (parameter variations) were made and the method of "harmonic balance" for finding these parameters was applied. It is shown that certain levels of excitation must be reached in order to make flight flutter tests reliable for establishing flutter clearance speeds. Some of the analytical work presented in this paper was sponsored by the ZTL-Research Program of the German Ministry of Defense.

INTRODUCTION

Nonlinearities and their effects are usually considered when dealing with aerospace structures, for many years. The introduction of airplanes with sweepable wings has stimulated increased interest as nonlinearities in this case are quite remarkable and effective on the general aircraft's dynamic behaviour and, therefore, on flutter (particularly the wing-store flutter case).

Adopting the terminology of Ref. 1, it is possible to distinguish between distributed and concentrated nonlinearities. The first case refers to the slightly nonlinear behaviour of complete structures, due to the nature of the internal damping of structural components and to the friction in their attachments, with rivets or other fasteners. The second case refers to the lumped sources of backlash and friction, leading to hysteresis type energy absorption, usually found in actuators and other items of control systems. The wing sweep-underwing stores alignment mechanical system discussed here represents the second case.

A schematic view of the system is given in Fig. 1 taken from Ref. 2. This system deserves further investigations because in this case, nonlinear effects cause, if a certain amplitude is exceeded, a complete change of the dynamic behaviour or, in other words, a change of the corresponding idealized spring-mass-damper representation, and, finally, a change of flutter characteristics. This can be explained using Fig. 2 which applies the same schematics as the test model of Ref. 2 to the real structure of a sweepable wing aircraft and refers exclusively to the store's and wing's symmetric yaw motion. At low amplitude, the store yaw motion is involving the pylon and wing fore and aft stiffnesses (the pylon behaves as if it was clamped to the wing). Exceeding a certain amplitude at which the friction preload in the pylon bearings is overcome, there is a relative motion of the pylon in respect to the wing, and also the control rod stiffness is involved after the backlash is exceeded.

Similarly in the wing pivot there is the possibility of a relative yaw motion of the wing in respect to the carry-through box structure if the friction is broken and the stiffness of the wing sweep actuation system is involved after the backlash is exceeded. The following paragraphs present the vibration and hysteresis measurements made on an existing aircraft and the corresponding analytical investigations. These are based on both the usual way to represent a nonlinear behaviour with different linear mathematical models and on the new method of setting up a single nonlinear mathematical model using the so called "harmonic balance".

GROUND RESONANCE TESTS RESULTS

After the small amplitude resonance tests quoted in Ref. 2, another series was done on a similar aircraft in which many powerful shakers were used in order to exceed the friction forces in the bearings of the wing-pylon attachment. Fig. 3 presents the results

obtained exciting the stores' symmetric yaw mode. The left part of the plot shows the usual frequency and damping trends due to small distributed nonlinearities. The pylon behaves as if it was clamped to the wing in the bearings. Fig. 4 shows the corresponding mode shape (mainly store pitch + store yaw), practically invariant in this range of amplitudes. The damping value (2 to 4 per cent of critical) is typical for materials and attachments with distributed fasteners.

After a certain increase of the input power, both frequency and damping values show a sudden and large variation revealing a completely different dynamic behaviour, confirmed also by the significant mode shape change (see Fig. 5). The pylon can now rotate in the bearings with a friction leading to a considerable energy loss as it is shown by the very high damping level (10 to 11 per cent). The mode is practically store yaw only.

The presence of a zone in which both behaviours can exist is explained the following way:

The two cases, having different mode shapes, require not only different input power but also different relative setting of the shakers to be properly excited. Conversely, it is possible to force each of the two behaviours for some while in the range in which the other response is expected, maintaining its proper shakers setting.

Similar nonlinearities affect also the stores pitch modes but the phenomenon is much more evident on yaw modes. Moreover, the wing store flutter is often mainly dominated by the coupling of these three symmetric modes: wing bending, store pitch, store yaw. A different relative frequency position of pitch and yaw modes like we have in the two ranges of Fig. 3 affects, therefore, the flutter mechanism.

LINEAR CALCULATIONS

To represent the two ranges, two linear mathematical models were set up according to the very simplified schematics of Fig. 6 which shows on the left side the clamped pylon case (rigid control rod) and on the right side the rotating pylon case (elastic control rod). The corresponding mode shapes for symmetric store yaw are shown in Fig. 4 and 5 in comparison with the previously mentioned experimental ones.

HYSTERESIS MEASUREMENTS

In order to set up a single nonlinear mathematical model, some hysteresis measurements were made on the same aircraft for the store yaw and wing yaw. The results are reported in Fig. 7 and 8. For the wing two cases were considered: the normal situation in which the wings generate friction forces in the pivot due to their weight and the case in which these forces are partially avoided, supporting part of the wings weight in such a way, to compensate the bending moment on the pivot.

ANALYTICAL INVESTIGATION OF STRUCTURAL NONLINEARITIES USING THE METHOD OF HARMONIC BALANCE

In principle, the measured force-deflection diagram with hysteresis (Fig. 9) which has to be represented in calculation is defined by the force necessary to overcome the static friction, the effective backlash and the nearly frictionless deformation at large force amplitudes.

For investigations discussed in this chapter, the calculations of nonlinear flutter boundaries are based on the method of the "harmonic balance" which was proved in Ref. 1 and 3 to be very suitable to represent the physical behaviour of nonlinear structures in conventional flutter calculations.

Fig. 10 illustrates in principle the linear approximation of hysteresis type deflection curves which has to be performed for different amplitudes. Assuming sinusoidal motions, the moment of force can be transformed to a periodical representation. The first harmonic is used to describe the equivalent linear stiffness coefficient $C(\beta)$ and damping loss angle $\gamma(\beta)$

$$C(\beta) = \frac{1}{\pi\beta} \int_{\varphi=0}^{2\pi} F(\beta\cos\varphi, -\beta\omega\sin\varphi)\cos\varphi \, d\varphi$$

$$\gamma(\beta) = \frac{1}{\pi\beta C(\beta)} \int_{\varphi=0}^{2\pi} F(\beta\cos\varphi, -\beta\omega\sin\varphi)\sin\varphi \, d\varphi$$

which can be introduced into conventional flutter calculations.

Results of flutter calculations, using this method, will be demonstrated now for three different cases of wing external store flutter. The stores are mounted on inboard and outboard pylon stations of a sweepable wing which incorporates backlash and friction in the wing pivot and also in the pylon bearings. The mechanism of flutter for the store configurations investigated here exhibits the wing bending-store pitch type of large wing mounted stores.

The first example is based on a configuration with inboard and outboard wing stores considering a nonlinear stiffness in the wing pivot yaw degree of freedom. The resonance modes which affect the flutter behaviour are depicted in Fig.11 . For the nominal linear wing pivot yaw stiffness as measured at large amplitudes, the wing yaw frequency is well separated from the store pitch mode, and the flutter conditions are defined only by the store pitch mode at 4.1 Hz and the wing bending mode at 3.47 Hz.

Measurements of the hysteresis curve and the moment of force-deflection diagram which were used for the harmonic approximation are shown in Fig. 12 whereas the equivalent linear stiffness and the equivalent damping loss angle as derived from the harmonic approximation are plotted in Fig.13 versus wing yaw amplitude. Starting with large stiffness and zero damping at small deflections, the stiffness reaches the lowest and the damping the largest value when the deflection achieves the hysteresis amplitude at $\beta = \beta_o$ (Fig. 14). At high amplitudes, the curves tend to the values of the linear system.

For amplitudes below the critical slip-stick point, the force-deflection curve is not well defined due to difficulties arising from stiffness measurements at very small amplitudes. In this case, it is assumed that more solid friction is effective at smaller amplitudes, and, therefore, the stiffness tends to infinite values at zero amplitude.

The results of flutter calculations, using the linearized coefficients of Fig.13 are plotted in Fig. 14 versus wing yaw amplitude. The lowest flutter speeds were found for very small and for very large amplitudes where the stiffness reaches about the linear value. In both cases, apparently no damping is introduced by the wing pivot yaw mode.

For amplitudes inside the hysteresis curve, high flutter speeds have been found which could either be explained by the influence of the hysteresis damping or by frequency changes of the wing yaw mode due to decreasing stiffness.

For comparison with the nonlinear flutter boundary, results of flutter calculations for the linear system but various wing pivot yaw stiffnesses are shown in Fig. 15 . Flutter points with corresponding values of wing yaw stiffness are marked with the letter A to D . Comparison of flutter speeds at equal stiffness values reveals that hysteresis damping of the wing yaw mode hardly affects the store pitch flutter.

Having a value of 6.5 Hz at 100 % stiffness, with decreasing stiffness the wing yaw frequency crosses the store pitch frequency of 4.1 Hz at about 43 % wing yaw stiffness (Point C) thus creating a change of the critical flutter mode resulting to high flutter speeds inside a certain region of wing yaw stiffness.

Although for this configuration the lowest possible flutter speed was found already by linear flutter calculations, the results are important in view of flight flutter testing, indicating that flight testing may not yield the lowest possible flutter speed if the flutter excitation is insufficient. These results could also indicate that the low flutter speed limits of linear calculation are not applicable if excitation amplitudes are required which are outside the design specifications.

By the second example, the influence of structural nonlinearities caused by the pylon bearing and store attachment are investigated on an inboard wing store configuration. The important modes involved in the store pitch flutter mechanism are depicted in Fig. 16 . Assuming linear stiffness, the frequency of the store yaw mode was found at 3.7 Hz. Fig.17 shows the measured hysteresis for the store yaw degree of freedom which has been introduced into the analysis.
Fig. 18 illustrates the results of the harmonic balance, and Fig. 19 shows the variation of the flutter speed with amplitude for the nonlinear structure whereas in Fig. 20 the results of a conventional flutter calculation are plotted for different values of store yaw stiffness.

Comparing flutter speeds obtained for linear and nonlinear stiffnesses, significant flutter conditions will be discussed now.

In both diagrams, the lowest flutterspeed is related to a very high stiffness value, marked by A . From the nonlinear plot, it can be seen that this large stiffness value is only existent for small amplitudes if a large amount of solid friction is assumed.

The nominal linear stiffness value (close to point B) is achieved twice in the nonlinear calculation at about $\beta/\beta_o = 0.5$ and $\beta = \infty$. Although there is a considerable amount of damping at the small amplitude $\beta/\beta_o = 0.5$, the nonlinear calculation results to similar flutterspeeds as obtained by the linear analysis. This proves that the hysteresis damping has only a minor influence due to the small coupling between store yaw and store pitch mode.

At the stiffness condition C ,the store pitch and store yaw mode are exchanging their characteristics thus causing high flutter speeds. The store yaw amplitude at this condition is close to the slip-stick amplitude which is related to zero damping. The linear and the nonlinear calculation, therefore, results to identical flutter speeds.

For the maximum damping condition at point D , the store yaw and store pitch frequencies are well separated which means that the hysteresis damping is not effective.

No structural damping has been considered in the nonlinear calculations for the store pitch mode. The effect of g = 2 % structural damping in the store pitch mode is shown by the results of linear flutter calculations in Fig. 20 .

From this investigations, it is obvious that significant influence of structural nonlinearities on the flutter behaviour can only be expected if the mode which exhibits the nonlinearities shows a strong coupling with the flutter mode at amplitudes inside the hysteresis or if the structural nonlinearity is related directly to the flutter mode. This case will be discussed by the next example.

No hysteresis measurements could be made available by test for the store pitch degree of freedom. A hysteresis curve was defined, therefore, using the largest possible value for the backlash in store pitch and assuming a realistic amount of friction. To account for uncertainties arising from the assumed amount of friction, the investigated moment of friction was varied from 30 % to 100 % as indicated in the hysteresis plot of Fig. 21.

To illustrate the influence of a nonlinear degree of freedom associated with the flutter mode, the same inboard store configuration was chosen as discussed in the preceeding example. From the frequency plot in Fig.22, as calculated for different amplitudes using equivalent linearised stiffnesses, it becomes obvious that the influence of the structural nonlinearity on flutter is primarily a stiffness effect. The wing bending frequency is matched at very small and at very high amplitudes, resulting in low flutter speeds. This is demonstrated by Fig.23 , showing the change of the flutter speed with variation of the store pitch amplitude. The low flutter speed at the smaller amplitude associated with zero damping is practically not important for flutter, because, according to the rapidly decreasing stiffness, it disappears if the amplitude is increased by small amounts. Assuming 30 % friction only, the loss in stiffness inside the hysteresis is even more violent, causing larger numbers of damping as indicated in Fig. 22 . But the flutter trend in Fig. 23 is almost unchanged due to identical values of linearised stiffness and zero damping in amplitude regions important for flutter.

Following the results of the calculations shown here, structural nonlinearities seem to have minor effect on the critical flutter speed because the lowest possible values occur always at the nominal linear stiffness related to large deflections. But these investigations also show that flutter margins obtained by flight testing could exhibit a considerable risk if sufficient amplitudes of excitation could not be reached. As shown by the flutter speed trend of Fig. 23 , an amplitude of at least 0.006 radians refering to about 1 g acceleration at the store nose is required to get safe flutter clearance speeds whereas in common flight testing, it is not always possible to achieve 1 g. It should be mentioned also that structural nonlinearities including hysteresis damping could be even more important in coherence with dynamic response problems and for flutter with limited amplitudes. Due to the level of amplitude usually being excited, the change of stiffness and damping inside the hysteresis can affect dynamic responses considerably.

FLIGHT TEST MEASUREMENTS

An example of different flutter behaviour is given by the curves in Fig. 24. They represent the critical mode damping versus airspeed measured in flight for a critical store configuration. The two recognizable trends correspond to two different excitation manoeuvres: longitudinal and lateral stick-jerks. The former gives a slightly higher flutter speed and is represented by the computed curve obtained with the linear mathematical model of the clamped pylon case. The latter, more critical one, fits better to the computed curve in which the linear model represents the case of the pylon free to rotate.

CONCLUSIONS

It could be confirmed by analytical and experimental results of flutter investigations that structural nonlinearities, involving hysteresis type damping, usually connect the most critical flutter with large amplitudes, describing the linear range of the stiffness distribution. In these cases, therefore, linear flutter calculations using large amplitude stiffnesses would be able to represent the most critical flutter condition.

As it was shown also, however, structural nonlinearities can create considerable problems if sufficiently large amplitudes are not achievable in flight flutter test and testing at low amplitudes would result to unsafe flutter clearance speeds. In these cases, nonlinear calculations using measured stiffness curves are indispensable, and the flutter clearance procedure has to be based on analytical results, using flight flutter test results for checking purposes only.

A low speed flutter condition at small amplitudes inside the hysteresis could generate flutter with limited amplitude thus creating fatigue problems rather than a stability problem.

REFERENCES

/1/ BREITBACH, E.
Effects of Structural Nonlinearities on Aircraft Vibration and Flutter
AGARD-Report 665 (1977)

/2/ HAIDL, G.
Nonlinear Effects in Aircraft Ground and Flight Vibration Tests
AGARD-Report 652 (1976)

/3/ SENSBURG, O.
SCHOEN, B.
Schwingungs- und Flatteranalyse von Flugzeugen mit besonderen nichtlinearen Struktureigenschaften
Zeitschr. f. Flugwissenschaften u. Weltraumforschung, No. 2 (1978), Heft 6

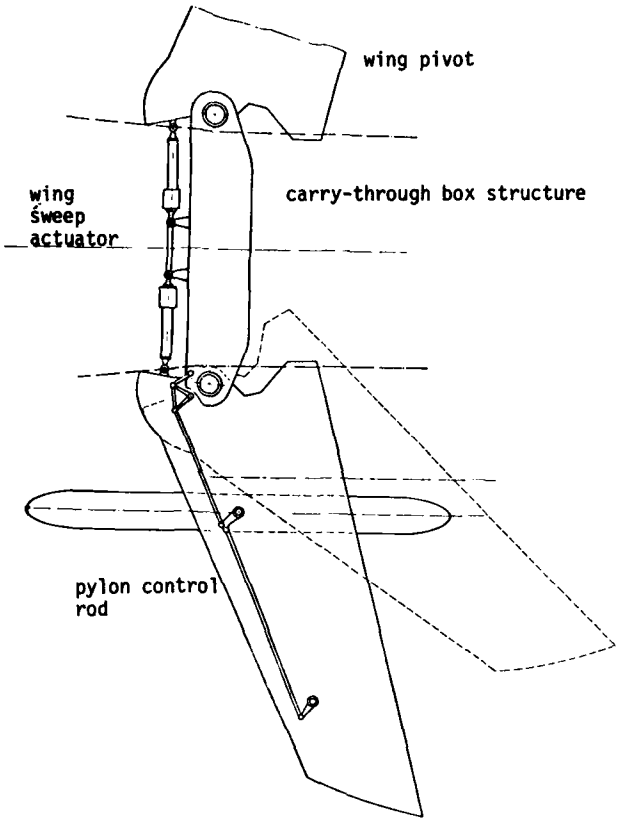

FIG. 1 SCHEMATIC VIEW OF THE WING SWEEP - UNDERWING STORES ALIGNMENT SYSTEM

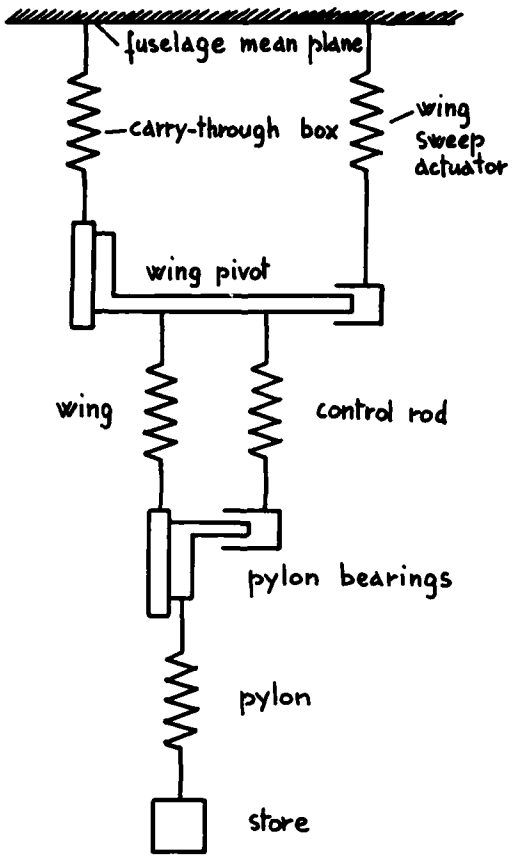

FIG. 2 IDEALIZED VIEW OF THE SYSTEM OF FIG. 1 FOR WING AND STORE YAW MOTION

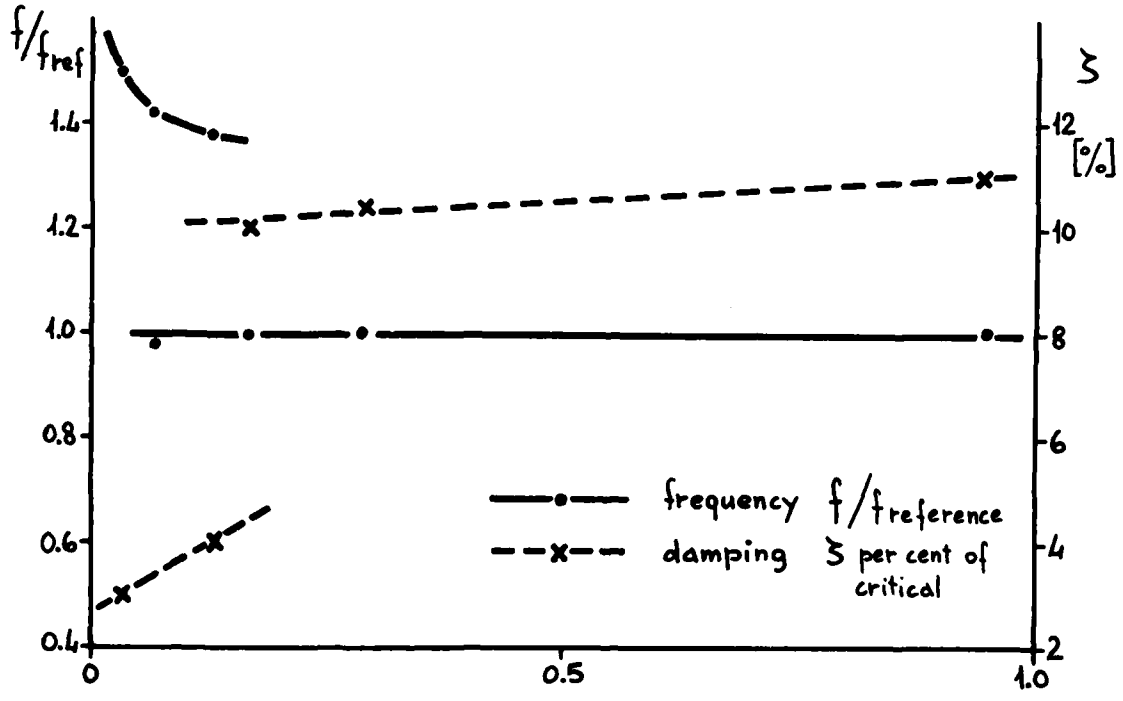

FIG. 3 STORE YAW FREQUENCY AND DAMPING TRENDS VERSUS INPUT POWER MEASURED DURING GROUND RESONANCE TESTS

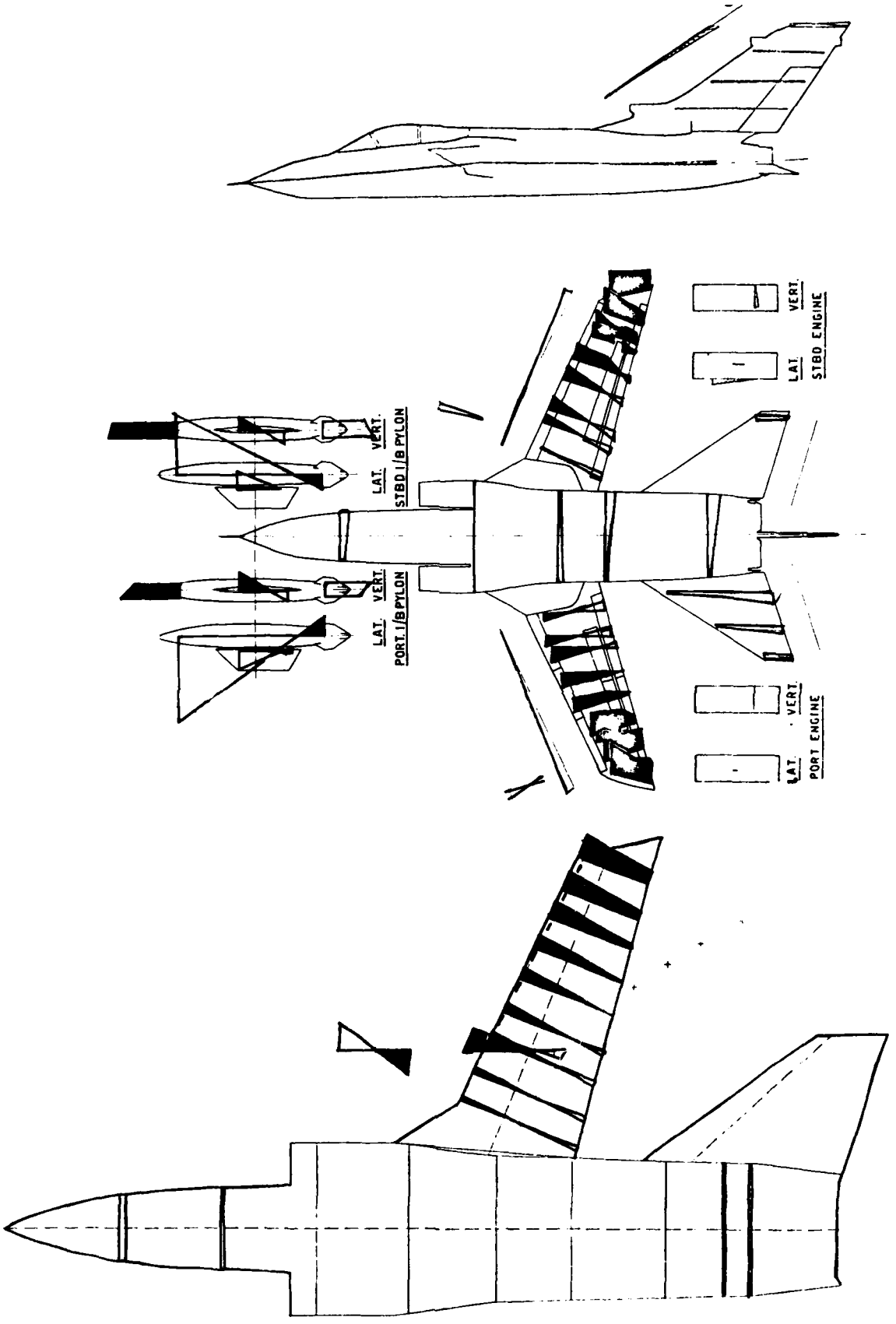

FIG. 4 STORE YAW MEASURED AND COMPUTED MODE SHAPE AT LOW AMPLITUDE

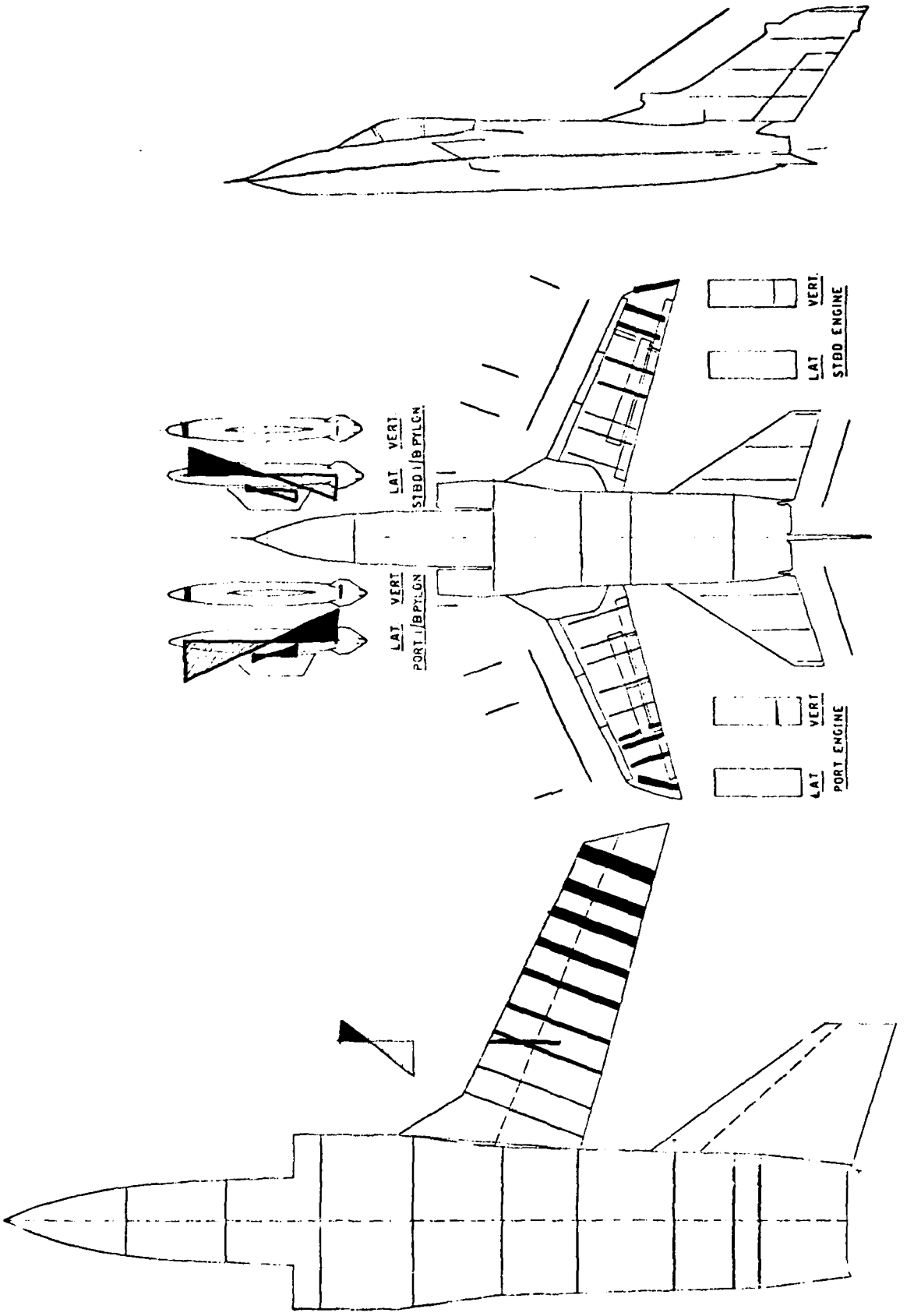

FIG. 5 STORE YAW - MEASURED AND COMPUTED MODE SHAPE AT LARGE AMPLITUDE

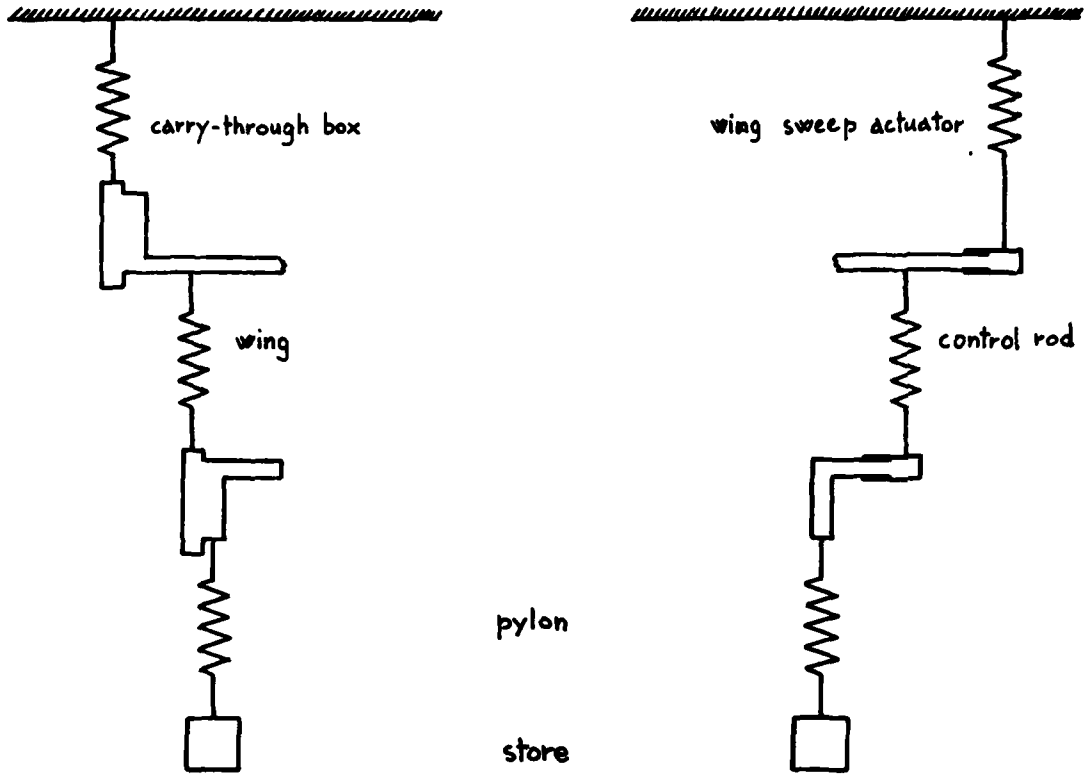

FIG. 6 SIMPLIFIED SCHEMATICS OF WING AND STORE YAW MOTION - LEFT: RIGID CONTROL ROD CASE - RIGHT: ELASTIC CONTROL ROD CASE

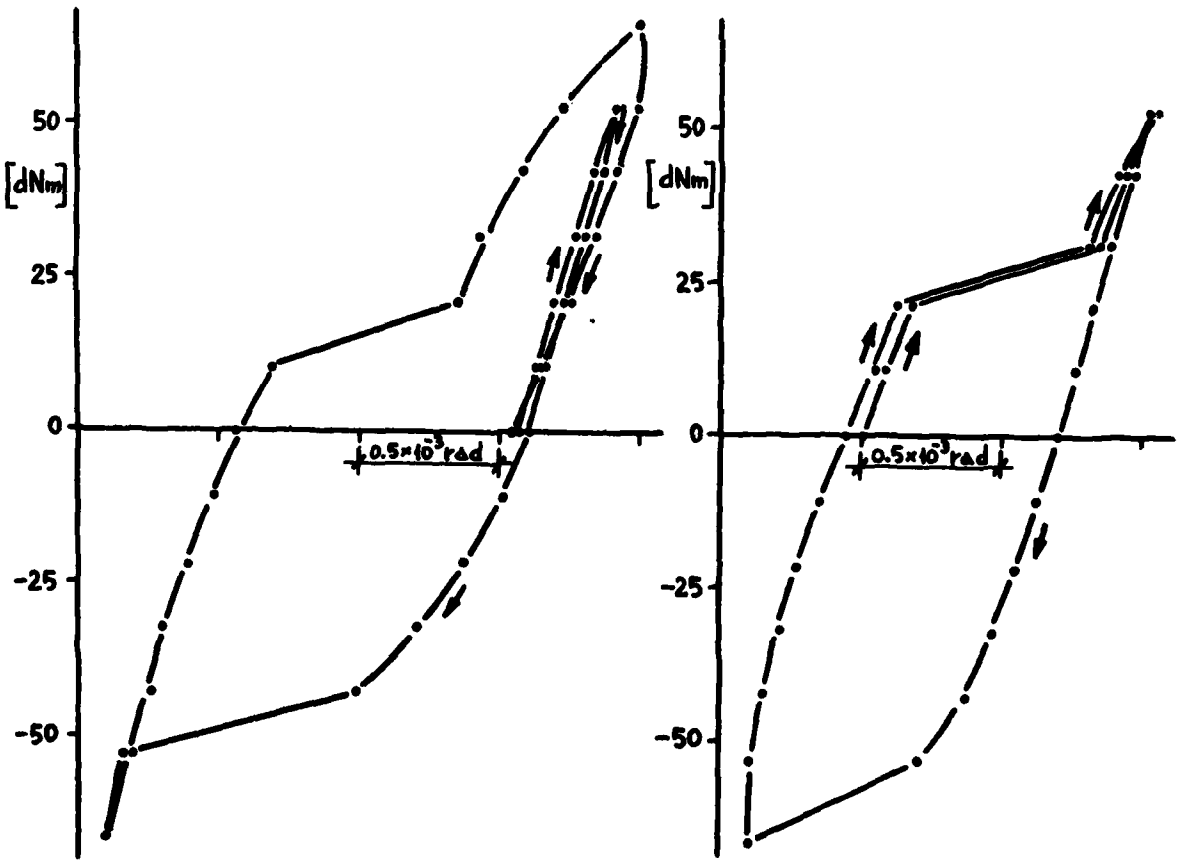

FIG. 7 STORE YAW HYSTERESIS TESTS - LEFT: PORT STORE - RIGHT: STARBOARD STORE

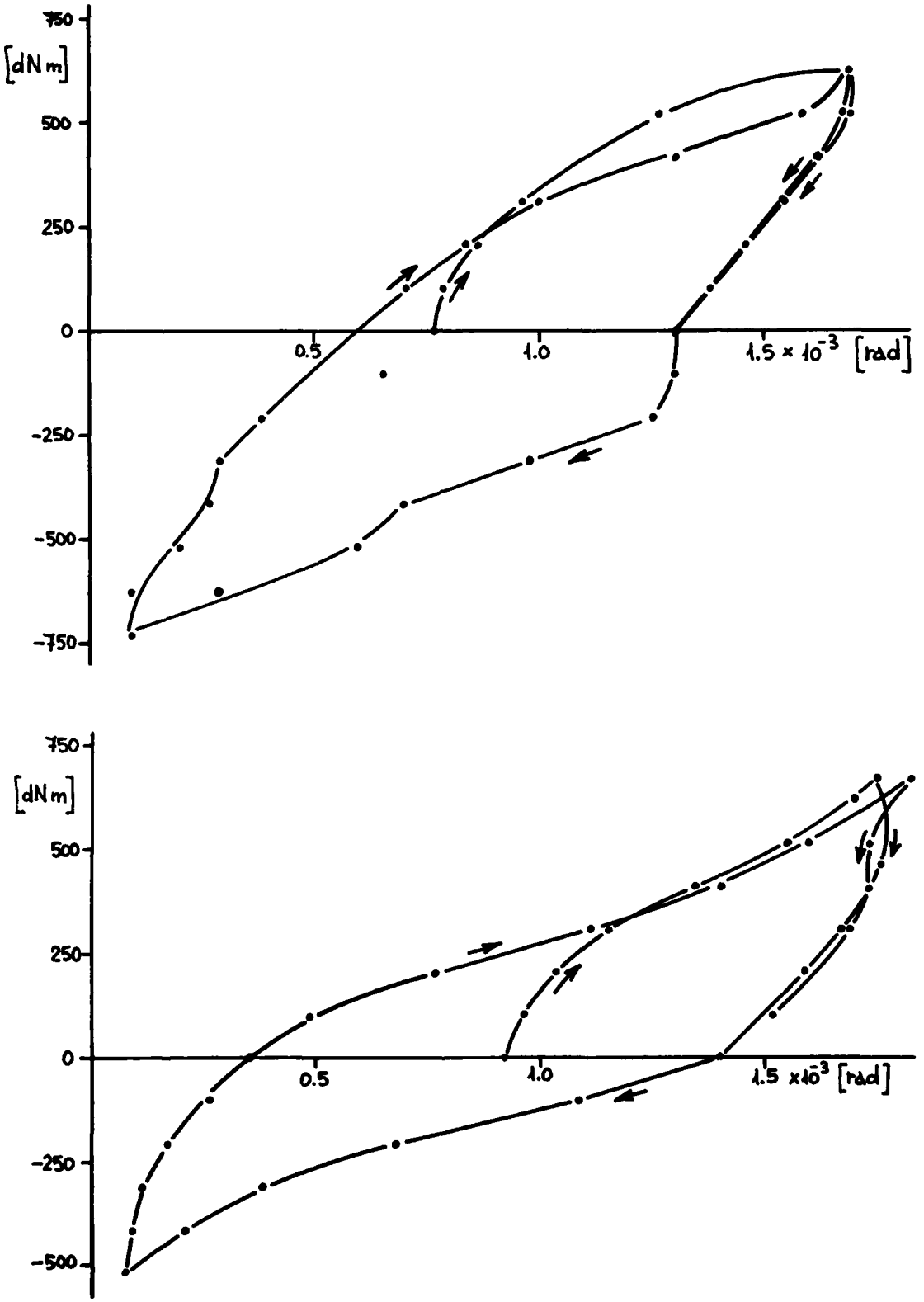

FIG. 8 WING YAW HYSTERESIS PLOTS

ABOVE : NORMAL
BELOW : WITH SUPPORTED WING

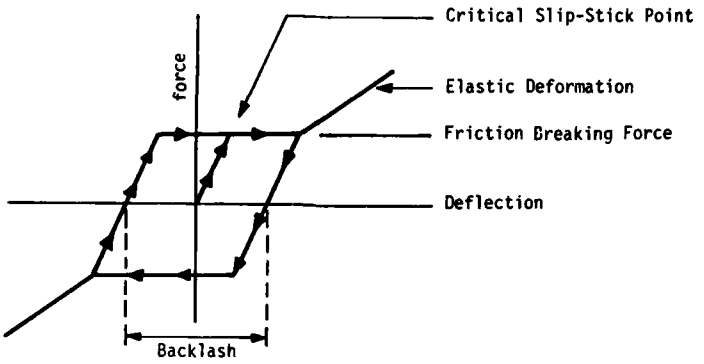

FIG. 9 SCHEMATIC HYSTERESIS DIAGRAM

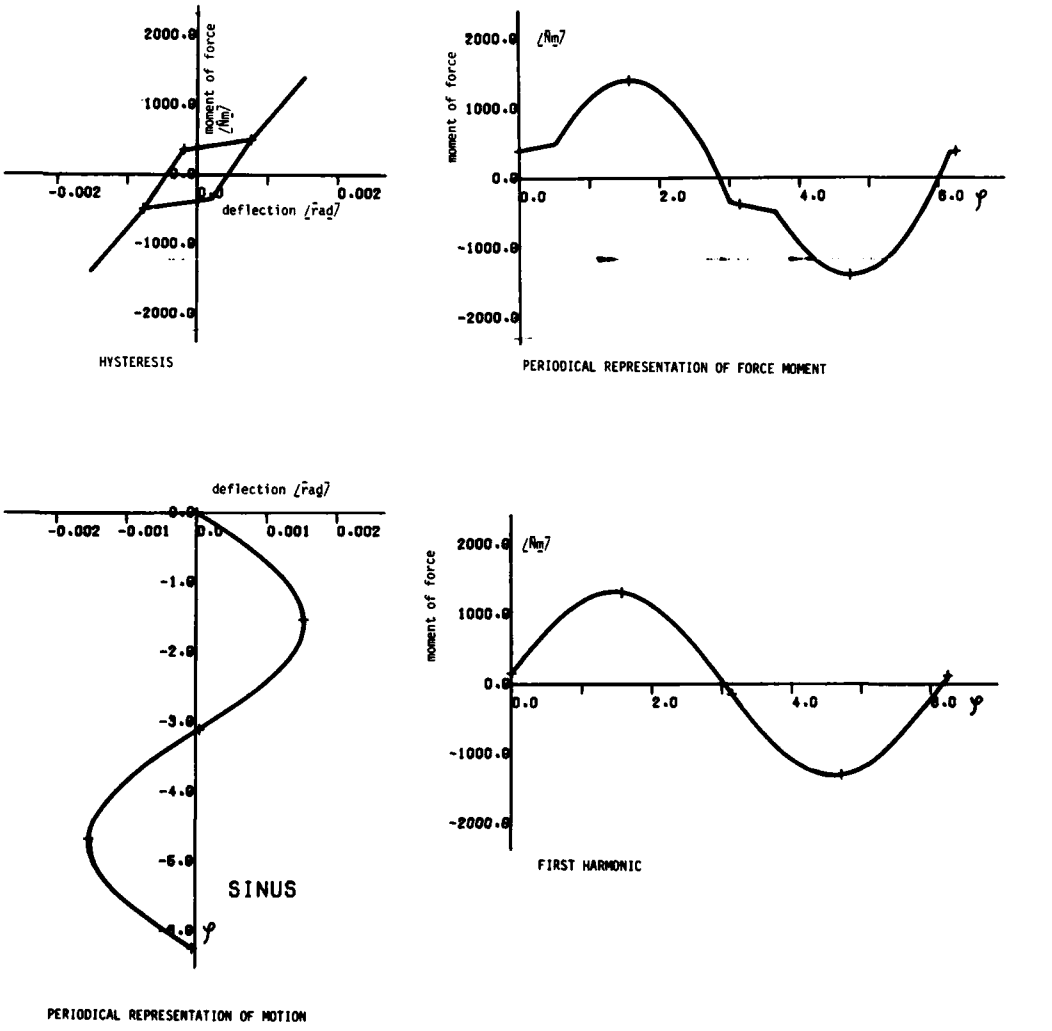

FIG.10 LINEARIZATION OF MEASURED DEFLECTION CURVES BY "HARMONIC BALANCE"

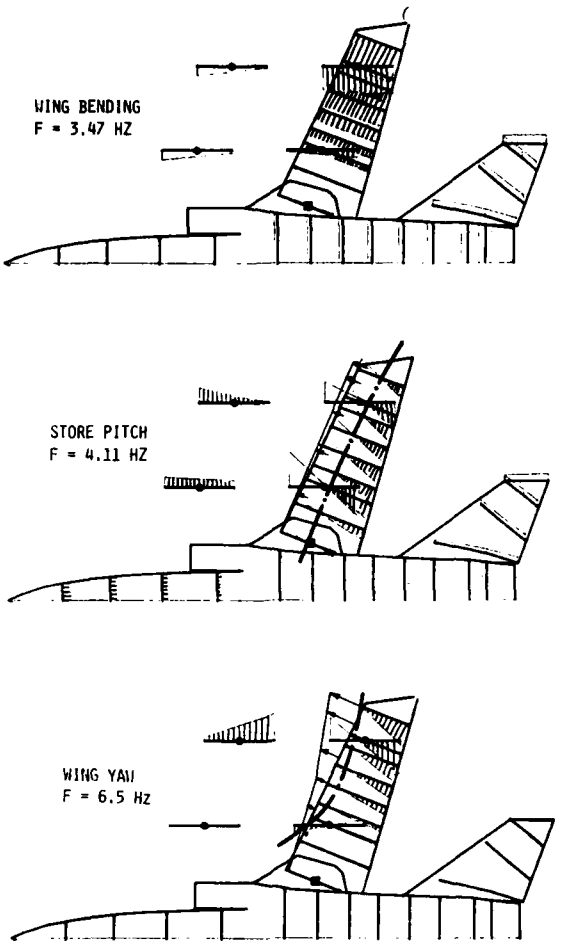

FIG.11 RESONANCE MODES OF A SWEEPABLE WING WITH INBOARD AND OUTBOARD STORES

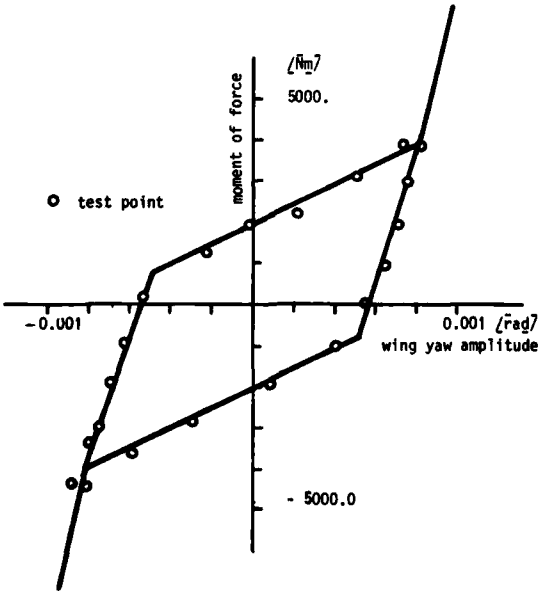

FIG.12 MEASURED HYSTERESIS CURVE OF WING PIVOT YAW DEFLECTIONS

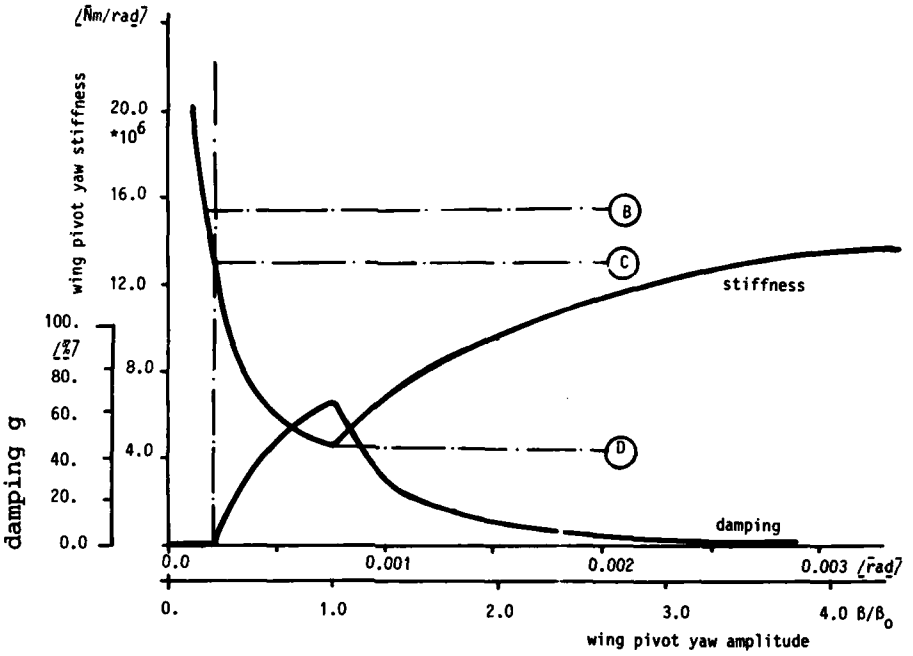

FIG.13 LINEARIZED STIFFNESS AND DAMPING LOSS ANGLE OF WING PIVOT YAW VERSUS WING YAW DEFLECTION

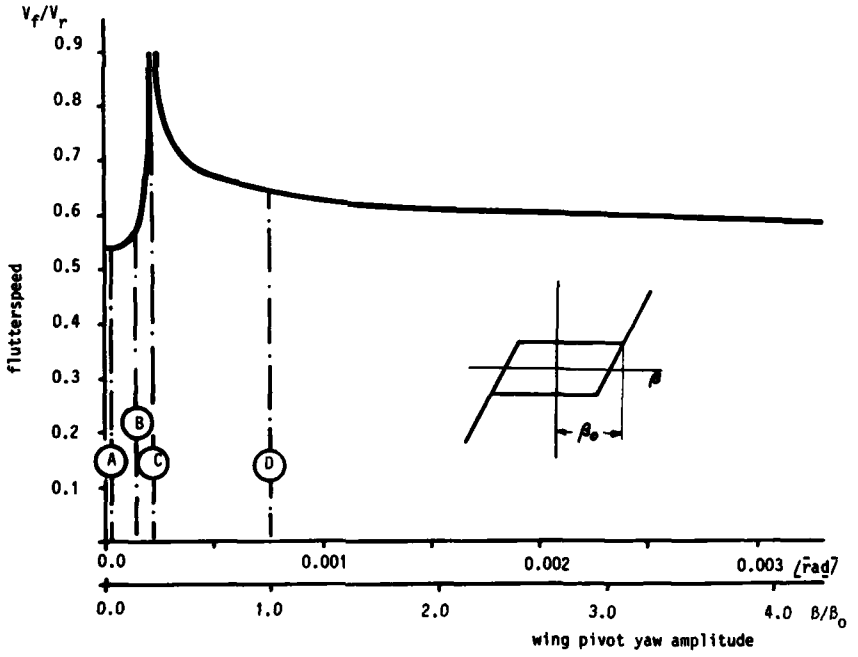

FIG.14 INFLUENCE OF WING PIVOT YAW AMPLITUDE ON THE FLUTTER SPEED OF INBOARD AND OUTBOARD WING STORES

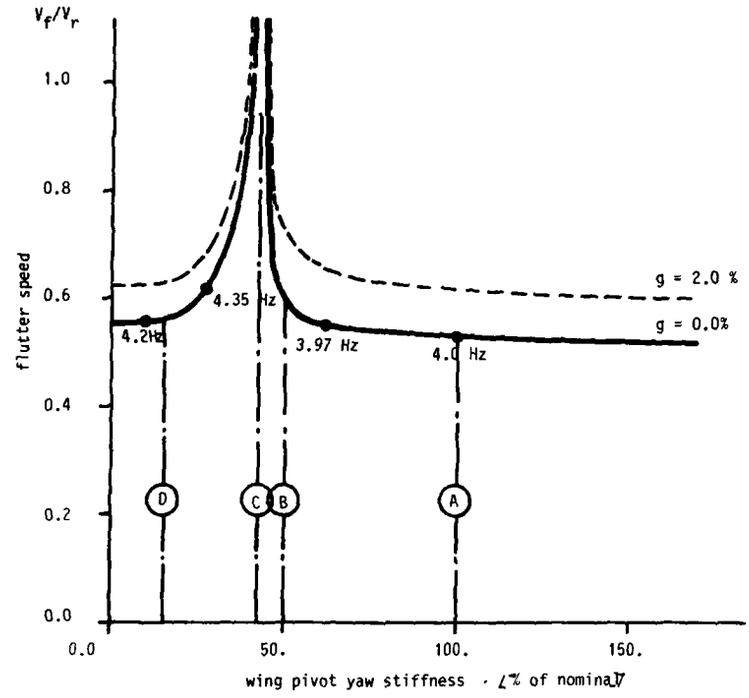

FIG.15 FLUTTER SPEED VERSUS WING PIVOT YAW STIFFNESS (CONVENTIONAL METHOD)

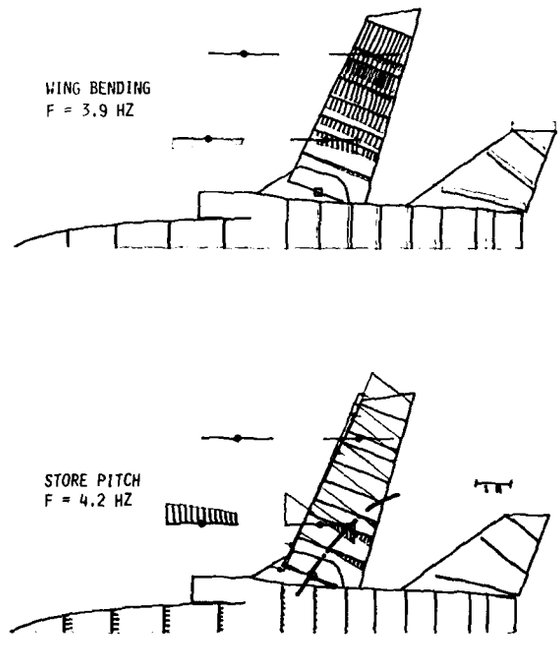

FIG.16 RESONANCE MODES OF A SWEEPABLE WING WITH INBOARD WING STORES

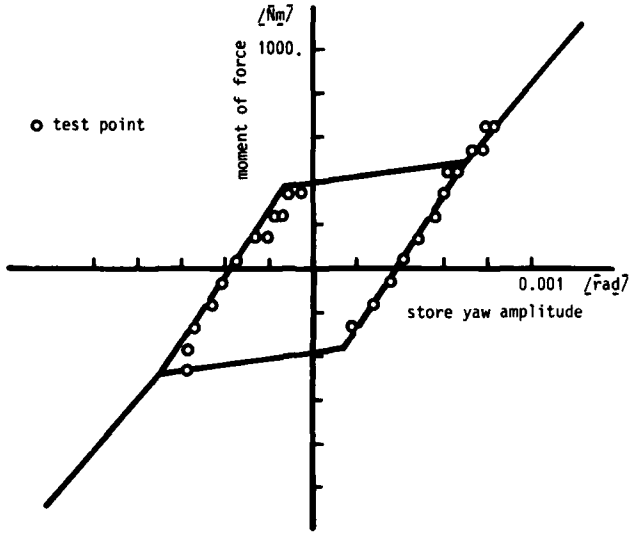

FIG.17 MEASURED HYSTERESIS CURVE OF INBOARD STORE YAW DEFLECTIONS

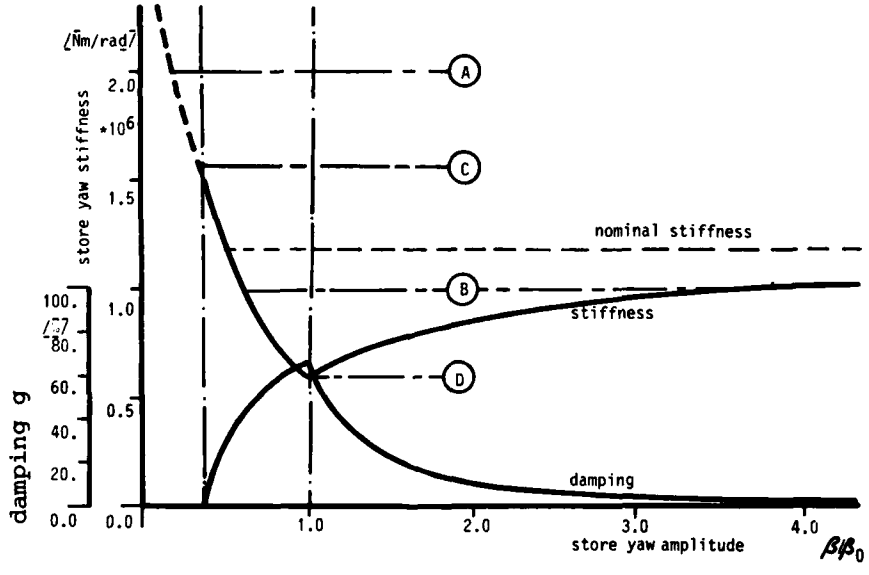

FIG.18 LINEARIZED STIFFNESS AND DAMPING LOSS ANGLE OF INBOARD STORE YAW VERSUS STORE YAW DEFLECTION

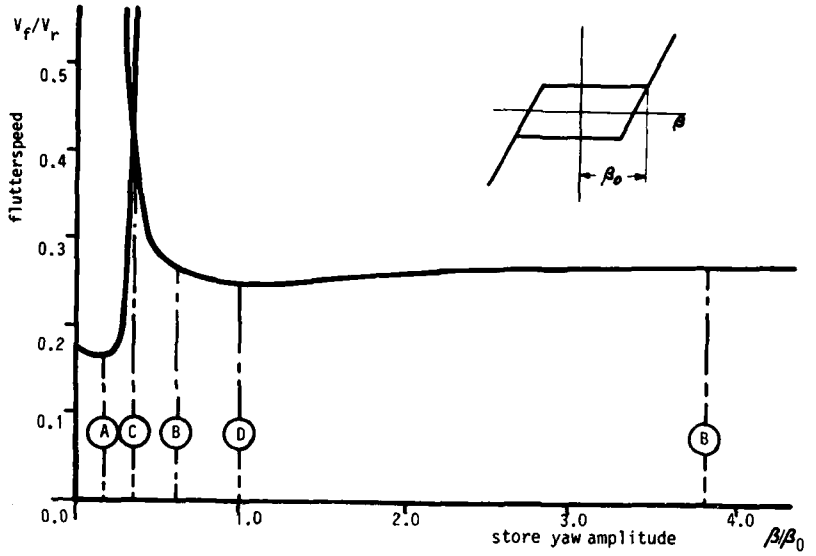

FIG.19 INFLUENCE OF INBOARD STORE YAW AMPLITUDE ON THE FLUTTER SPEED OF INBOARD WING STORES

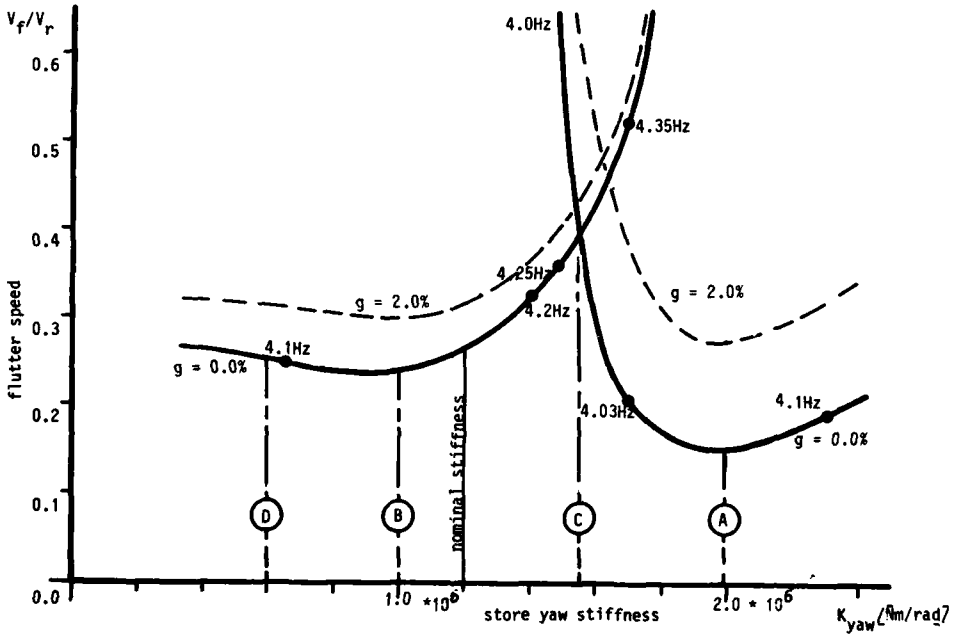

FIG.20 FLUTTER SPEED VERSUS INBOARD STORE YAW STIFFNESS (CONVENTIONAL METHOD)

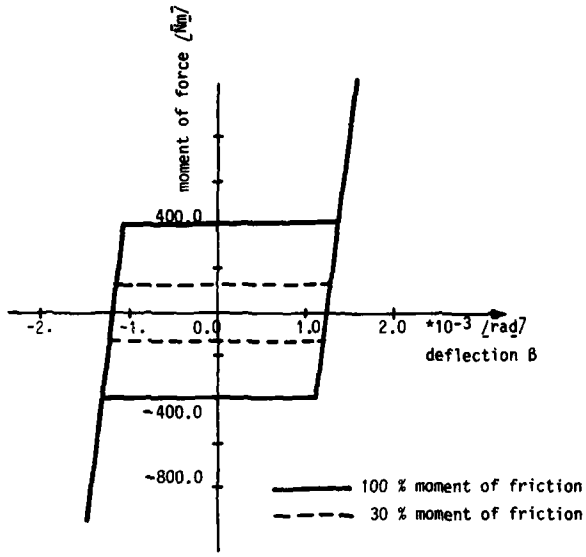

FIG.21 HYSTERESIS CURVE OF INBOARD STORE PITCH DEFLECTIONS DERIVED FROM DESIGN CONSIDERATIONS

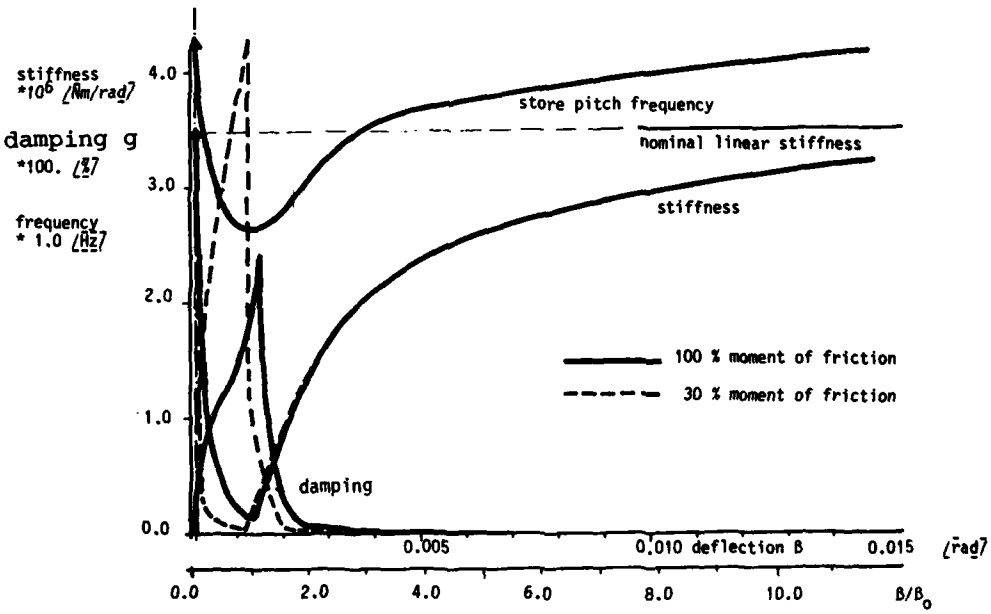

FIG.22 LINEARIZED STIFFNESS AND DAMPING LOSS ANGLE OF INBOARD STORE PITCH VERSUS STORE PITCH DEFLECTION

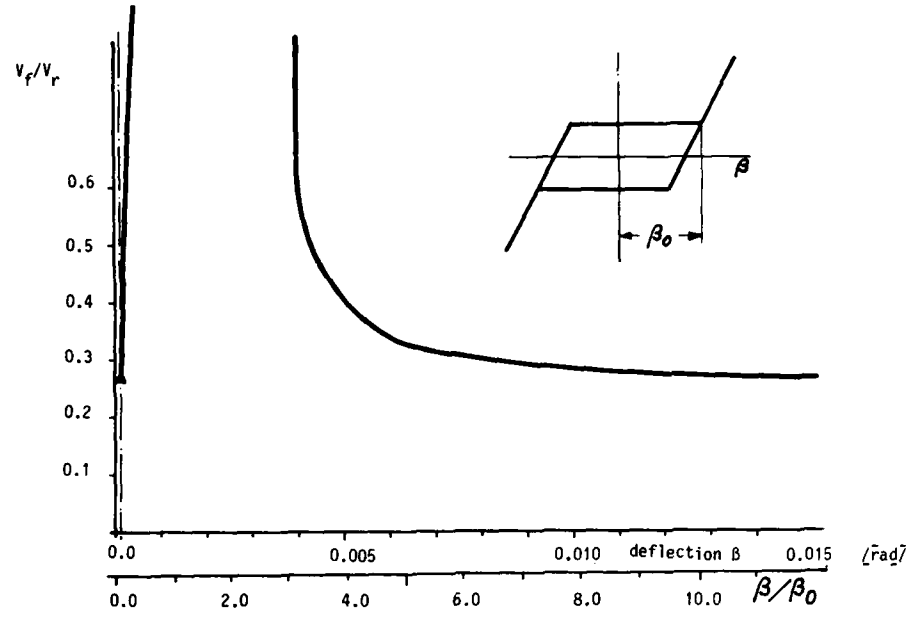

FIG.23 INFLUENCE OF INBOARD STORE PITCH AMPLITUDE ON THE FLUTTER SPEED OF INBOARD WING STORES

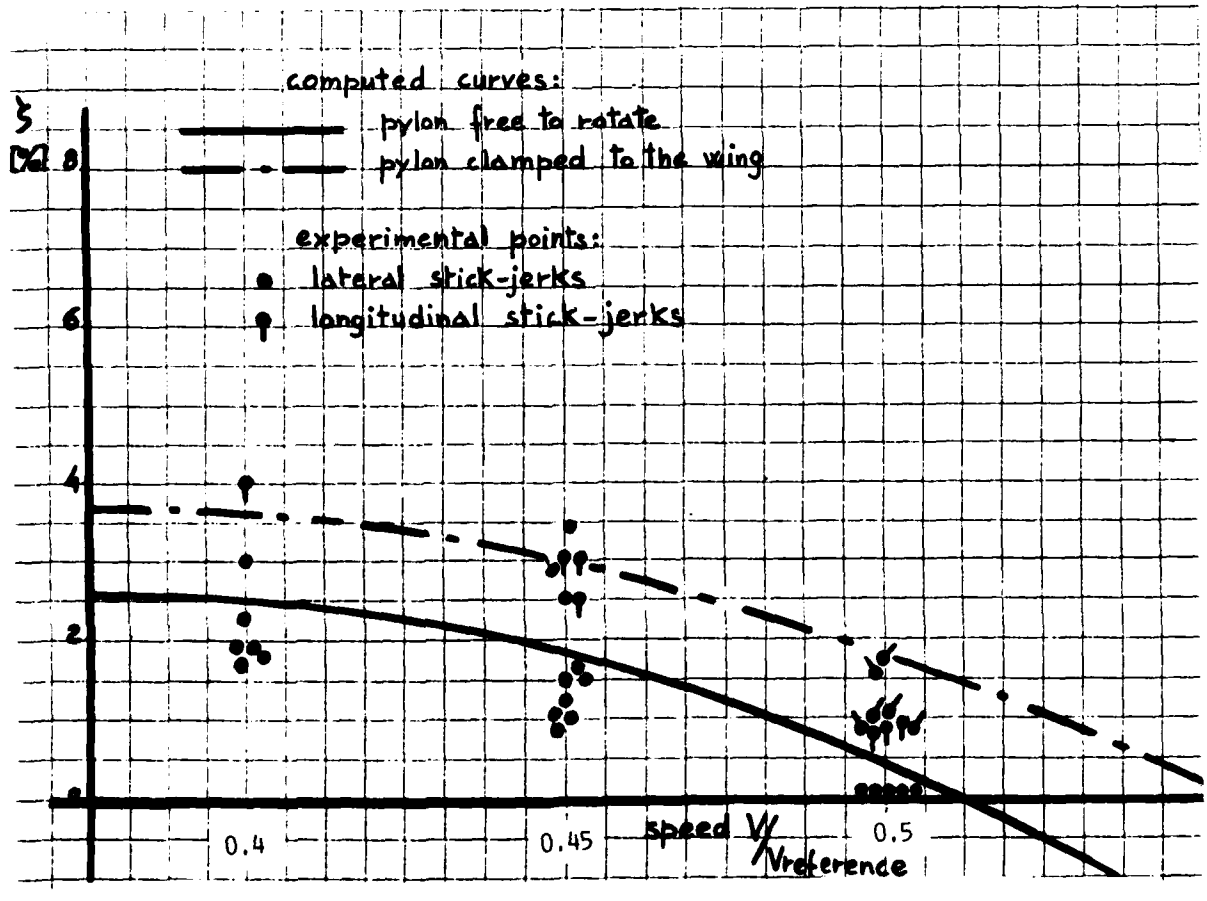

FIG 24 IN FLIGHT MEASURED DAMPING VALUES COMPARED WITH COMPUTED CURVES INBOARD AND OUTBOARD WING STORES

REPORT DOCUMENTATION PAGE

1. Recipient's Reference	2. Originator's Reference	3. Further Reference	4. Security Classification of Document
	AGARD-R-687	ISBN 92-835-1365-7	UNCLASSIFIED

5. Originator Advisory Group for Aerospace Research and Development
North Atlantic Treaty Organization
7 rue Ancelle, 92200 Neuilly sur Seine, France

6. Title MATHEMATICAL MODELING OF LINEAR AND NON-LINEAR AIRCRAFT STRUCTURES

7. Presented at

8. Author(s)/Editor(s)	9. Date
Various	July 1980
10. Author's/Editor's Address	**11. Pages**
Various	38

12. Distribution Statement This document is distributed in accordance with AGARD policies and regulations, which are outlined on the Outside Back Covers of all AGARD publications.

13. Keywords/Descriptors

Mathematical models
Aeroelasticity
Flutter
Aerodynamic configurations
Airframes
Wings
External stores

14. Abstract

This report comprises two papers presented to the Aeroelasticity Sub-Committee of the Structures and Materials Panel in April 1980. One paper proposes adjustment algorithms for improving the theoretically obtained flexibility and mass distributions of an aircraft structure by dynamic or ground resonance tests. The other deals with the non-linear behaviour of wing-store configurations and its analytical representation. Conclusions are drawn on the excitation amplitudes at which flutter could occur.

This report was prepared at the request of the Structures and Materials Panel of AGARD.

AGARD Report No.687 Advisory Group for Aerospace Research and Development, NATO MATHEMATICAL MODELING OF LINEAR AND NON-LINEAR AIRCRAFT STRUCTURES Published July 1980 38 pages This report comprises two papers presented to the Aeroelasticity Sub-Committee of the Structures and Materials Panel in April 1980. One paper proposes adjustment algorithms for improving the theoretically obtained flexibility and mass distributions of an aircraft structure by dynamic or ground resonance tests. The other deals with the non-linear behaviour of wing-store P.T.O.	AGARD-R-687 Mathematical models Aeroelasticity Flutter Aerodynamic configurations Airframes Wings External stores	AGARD Report No.687 Advisory Group for Aerospace Research and Development, NATO MATHEMATICAL MODELING OF LINEAR AND NON-LINEAR AIRCRAFT STRUCTURES Published July 1980 38 pages This report comprises two papers presented to the Aeroelasticity Sub-Committee of the Structures and Materials Panel in April 1980. One paper proposes adjustment algorithms for improving the theoretically obtained flexibility and mass distributions of an aircraft structure by dynamic or ground resonance tests. The other deals with the non-linear behaviour of wing-store P.T.O.	AGARD-R-687 Mathematical models Aeroelasticity Flutter Aerodynamic configurations Airframes Wings External stores
AGARD Report No.687 Advisory Group for Aerospace Research and Development, NATO MATHEMATICAL MODELING OF LINEAR AND NON-LINEAR AIRCRAFT STRUCTURES Published July 1980 38 pages This report comprises two papers presented to the Aeroelasticity Sub-Committee of the Structures and Materials Panel in April 1980. One paper proposes adjustment algorithms for improving the theoretically obtained flexibility and mass distributions of an aircraft structure by dynamic or ground resonance tests. The other deals with the non-linear behaviour of wing-store P.T.O.	AGARD-R-687 Mathematical models Aeroelasticity Flutter Aerodynamic configurations Airframes Wings External stores	AGARD Report No.687 Advisory Group for Aerospace Research and Development, NATO MATHEMATICAL MODELING OF LINEAR AND NON-LINEAR AIRCRAFT STRUCTURES Published July 1980 38 pages This report comprises two papers presented to the Aeroelasticity Sub-Committee of the Structures and Materials Panel in April 1980. One paper proposes adjustment algorithms for improving the theoretically obtained flexibility and mass distributions of an aircraft structure by dynamic or ground resonance tests. The other deals with the non-linear behaviour of wing-store P.T.O.	AGARD-R-687 Mathematical models Aeroelasticity Flutter Aerodynamic configurations Airframes Wings External stores

configurations and its analytical representation. Conclusions are drawn on the excitation amplitudes at which flutter could occur. This report was prepared at the request of the Structures and Materials Panel of AGARD. ISBN 92-835-1365-7	configurations and its analytical representation. Conclusions are drawn on the excitation amplitudes at which flutter could occur. This report was prepared at the request of the Structures and Materials Panel of AGARD. ISBN 92-835-1365-7
configurations and its analytical representation. Conclusions are drawn on the excitation amplitudes at which flutter could occur. This report was prepared at the request of the Structures and Materials Panel of AGARD. ISBN 92-835-1365-7	configurations and its analytical representation. Conclusions are drawn on the excitation amplitudes at which flutter could occur. This report was prepared at the request of the Structures and Materials Panel of AGARD. ISBN 92-835-1365-7